

**KINETIC EFFECT OF ALKYLATED LINEAR AMINE
LIGANDS IN HOMOGENEOUS ATOM TRANSFER
RADICAL POLYMERIZATION**

**M. Sc. Thesis by
Hasan Alper ONDUR**

**Department: Polymer Science and Technology
Programme: Polymer Science and Technology**

Supervisor: Prof.Dr. Metin H. ACAR

JUNE 2005

**KINETIC EFFECT OF ALKYLATED LINEAR AMINE
LIGANDS IN HOMOGENOUS ATOM TRANSFER
RADICAL POLYMERIZATION**

**M. Sc. Thesis by
Hasan Alper ONDUR
(515031018)**

Date of submission: 9 May 2005

Date of defence examination: 2 June 2005

Supervisor (Chairman): Prof.Dr. Metin H. ACAR

Members of the Examining Committee: Prof.Dr. Yusuf YAĞCI (İTÜ)

Assist.Prof.Dr. Ersin ACAR (BÜ)

JUNE 2005

**ALKİLENMİŞ LİNEER AMİN LİGANDLARIN
HOMOJEN ATOM TRANSFER RADİKAL
POLİMERİZASYONUNA KİNETİK ETKİLERİ**

YÜKSEK LİSANS TEZİ

Hasan Alper ONDUR

(515031018)

Tezin Enstitüye Verildiği Tarih: 9 Mayıs 2005

Tezin Savunulduğu Tarih: 2 Haziran 2005

Tez Danışmanı: Prof.Dr. Metin H. ACAR

Diğer Jüri Üyeleri: Prof.Dr. Yusuf YAĞCI (İTÜ)

Yrd.Doç.Dr. Ersin ACAR (BÜ)

HAZİRAN 2005

ACKNOWLEDGEMENT

This master study has been carried out at Istanbul Technical University, Chemistry Department of Science & Letters Faculty.

I would like to express my gratitude to my supervisor Prof. Dr. Metin H. ACAR for offering invaluable help in all possible ways, continuous encouragement and helpful critics throughout this research.

I would like to thank Prof. Dr. Yusuf YAĞCI, Prof. Dr. Gürkan HIZAL and Prof. Dr. Ümit TUNCA for their help and discussion during my project.

I especially thank Şebnem İNCEOĞLU, Tuba ERDOĞAN, Hümeyra MERT, Hakan DURMAZ for their friendly, helpful attitude, their tolerance with me and patience during my laboratory works.

I am also grateful to my family and my friends Çağlar Remzi BECER and Yasemin YILDIZ for their patience, understanding and moral support during all stages involved in the preparation of this research.

May 2005

Hasan Alper ONDUR

TABLE OF CONTENTS

LIST OF ABBREVIATIONS	v
LIST OF TABLES	vi
LIST OF FIGURES	vii
LIST OF SYMBOLS	x
SUMMARY	xi
ÖZET	xii
1. INTRODUCTION	1
2. THEORETICAL PART	2
2.1. Conventional Free Radical Polymerizations	3
2.2. Controlled/"Living" Radical Polymerization	4
2.2.1. Atom Transfer Radical Polymerization (ATRP)	6
2.2.1.1. Monomers	7
2.2.1.2. Initiators	7
2.2.1.3. Ligands	8
2.2.1.4. Transition Metal Complexes	11
2.2.1.5. Solvents	11
2.2.1.6. Kinetics of ATRP	11
3. EXPERIMENTAL PART	15
3.1. Chemicals	15
3.2. Polymerization of Styrene	15
3.3. Polymerization of Methyl Methacrylate	16
3.4. Characterization	16
4. RESULTS AND DISCUSSION	17
4.1. ATRP of Styrene	17
4.1.1. Using 1,1,4,7,7-pentaethyldiethylenetriamine (PEDETA)	17
4.1.2. Using 1,1,4,7,7-pentabutyldiethylenetriamine (PBDETA)	19
4.1.3. Using 1,1,4,7,7-pentahexyldiethylenetriamine (PHDETA)	20
4.1.4. Using 1,1,4,7,10,10-hexaethyltriethylenetetramine (HETETA)	22
4.1.5. Using 1,1,4,7,10,10-hexabutyltriethylenetetramine (HBTETA)	23
4.1.6. Using 1,1,4,7,10,10-hexahexyltriethylenetetramine (HHTETA)	25
4.1.7. Using 1,1,4,7,7-pentamethyldiethylenetriamine (PMDETA)	26
4.1.8. Using bipyridine (bpy)	28
4.1.9. Using dinonylbipyridine (dNbpy)	29
4.1.10. Using tris(2-(dimethylamino)-ethyl)amine (Me ₆ -TREN)	31
4.2. Results for ATRP of Styrene	32
4.3. ATRP of Methyl Methacrylate	34
4.3.1. Using 1,1,4,7,7-pentaethyldiethylenetriamine (PEDETA)	34
4.3.2. Using 1,1,4,7,7-pentabutyldiethylenetriamine (PBDETA)	36
4.3.3. Using 1,1,4,7,7-pentahexyldiethylenetriamine (PHDETA)	37

4.3.4. Using 1,1,4,7,10,10-hexaethyltriethylenetetramine (HETETA)	39
4.3.5. Using 1,1,4,7,10,10-hexabutyltriethylenetetramine (HBTETA)	40
4.3.6. Using 1,1,4,7,10,10-hexahexyltriethylenetetramine (HHTETA)	42
4.3.7. Using 1,1,4,7,7-pentamethyldiethylenetriamine (PMDETA)	43
4.3.8. Using bipyridine (bpy)	45
4.3.9. Using dinonylbipyridine (dNbpy)	46
4.3.10. Using tris(2-(dimethylamino)-ethyl)amine (Me ₆ -TREN)	48
4.4. Results for ATRP of Methyl Methacrylate	49
4.5. Comparison of Ligands	51
5. CONCLUSION AND RECOMENDATIONS	54
REFERENCES	55
AUTOBIOGRAPHY	59

LIST OF ABBREVIATIONS

M_n	: Number average molecular weight of polymer
M_w	: Weight average molecular weight of polymer
MMA	: Methyl methacrylate
St	: Styrene
I, M	: Initiator and monomer respectively
PMDETA	: <i>N,N,N',N'',N'''</i> -(pentamethyldiethylenetriamine)
PDI	: Polydispersity index
EiBB	: Ethyl-2-bromoisobutyrate
EBP	: Ethyl-2-bromopropionate

LIST OF TABLES

	<u>Page No</u>
Table 2.1. The most frequently used initiator types in ATRP systems	8
Table 4.1. Results for ATRP of St in carried out experiments	33
Table 4.2. Results for ATRP of MMA in carried out experiments	50

LIST OF FIGURES

	<u>Page No</u>
Figure 2.1 : Kinetic plot and conversion vs. time plot for ATRP.....	12
Figure 4.1 : Semi-logarithmic kinetic plot for ATRP of St using PEDETA as a ligand.....	18
Figure 4.2 : Molecular weight and molecular weight distribution <i>versus</i> conversion plot for ATRP of St using PEDETA.....	18
Figure 4.3 : Semi-logarithmic kinetic plot for ATRP of St using PBDETA as a ligand.....	19
Figure 4.4 : Molecular weight and molecular weight distribution <i>versus</i> conversion plot for ATRP of St using PBDETA	20
Figure 4.5 : Semi-logarithmic kinetic plot for ATRP of St using PHDETA as a ligand.....	21
Figure 4.6 : Molecular weight and molecular weight distribution <i>versus</i> conversion plot for ATRP of St using PHDETA	21
Figure 4.7 : Semi-logarithmic kinetic plot for ATRP of St using HETETA as a ligand.....	22
Figure 4.8 : Molecular weight and molecular weight distribution <i>versus</i> conversion plot for ATRP of St using HETETA	23
Figure 4.9 : Semi-logarithmic kinetic plot for ATRP of St using HBTETA as a ligand.....	24
Figure 4.10 : Molecular weight and molecular weight distribution <i>versus</i> conversion plot for ATRP of St using HBTETA	24
Figure 4.11 : Semi-logarithmic kinetic plot for ATRP of St using HHTETA as a ligand.....	25
Figure 4.12 : Molecular weight and molecular weight distribution <i>versus</i> conversion plot for ATRP of St using HHTETA	26
Figure 4.13 : Semi-logarithmic kinetic plot for ATRP of St using PMDETA as a ligand.....	27
Figure 4.14 : Molecular weight and molecular weight distribution <i>versus</i> conversion plot for ATRP of St using PMDETA	27
Figure 4.15 : Semi-logarithmic kinetic plot for ATRP of St using bpy as a ligand.....	28

Figure 4.16 : Molecular weight and molecular weight distribution <i>versus</i> conversion plot for ATRP of St using bpy	29
Figure 4.17 : Semi-logarithmic kinetic plot for ATRP of St using dNbpy as a ligand.....	30
Figure 4.18 : Molecular weight and molecular weight distribution <i>versus</i> conversion plot for ATRP of St using dNbpy	30
Figure 4.19 : Semi-logarithmic kinetic plot for ATRP of St using Me ₆ -TREN as a ligand.....	31
Figure 4.20 : Molecular weight and molecular weight distribution <i>versus</i> conversion plot for ATRP of St using Me ₆ -TREN	32
Figure 4.21 : Semi-logarithmic kinetic plot for ATRP of MMA using PEDETA as a ligand	35
Figure 4.22 : Molecular weight and molecular weight distribution <i>versus</i> conversion plot for ATRP of MMA using PEDETA	35
Figure 4.23 : Semi-logarithmic kinetic plot for ATRP of MMA using PBDETA as a ligand	36
Figure 4.24 : Molecular weight and molecular weight distribution <i>versus</i> conversion plot for ATRP of MMA using PBDETA	37
Figure 4.25 : Semi-logarithmic kinetic plot for ATRP of MMA using PHDETA as a ligand	38
Figure 4.26 : Molecular weight and molecular weight distribution <i>versus</i> conversion plot for ATRP of MMA using PHDETA	38
Figure 4.27 : Semi-logarithmic kinetic plot for ATRP of MMA using HETETA as a ligand	39
Figure 4.28 : Molecular weight and molecular weight distribution <i>versus</i> conversion plot for ATRP of MMA using HETETA	40
Figure 4.29 : Semi-logarithmic kinetic plot for ATRP of MMA using HBTETA as a ligand	41
Figure 4.30 : Molecular weight and molecular weight distribution <i>versus</i> conversion plot for ATRP of MMA using HBTETA	41
Figure 4.31 : Semi-logarithmic kinetic plot for ATRP of MMA using HHTETA as a ligand	42
Figure 4.32 : Molecular weight and molecular weight distribution <i>versus</i> conversion plot for ATRP of MMA using HHTETA	43

Figure 4.33 : Semi-logarithmic kinetic plot for ATRP of MMA using PMDETA as a ligand	44
Figure 4.34 : Molecular weight and molecular weight distribution <i>versus</i> conversion plot for ATRP of MMA using PMDETA	44
Figure 4.35 : Semi-logarithmic kinetic plot for ATRP of MMA using bpy as a ligand	45
Figure 4.36 : Molecular weight and molecular weight distribution <i>versus</i> conversion plot for ATRP of MMA using bpy	46
Figure 4.37 : Semi-logarithmic kinetic plot for ATRP of MMA using dNbpy as a ligand	47
Figure 4.38 : Molecular weight and molecular weight distribution <i>versus</i> conversion plot for ATRP of MMA using dNbpy	47
Figure 4.39 : Semi-logarithmic kinetic plot for ATRP of MMA using Me ₆ -TREN as a ligand	48
Figure 4.40 : Molecular weight and molecular weight distribution <i>versus</i> conversion plot for ATRP of MMA using Me ₆ -TREN	49
Figure 4.41 : Semi-logarithmic kinetic plot for ATRP of MMA using PMDETA, PEDETA, HETETA as ligand	51
Figure 4.42 : Semi-logarithmic kinetic plot for ATRP of St using PMDETA, PEDETA, HETETA as ligand	52
Figure 4.43 : Semi-logarithmic kinetic plot for ATRP of St using Me ₆ -TREN, PEDETA, HETETA as ligand	53

LIST OF SYMBOLS

- M_n : Number average molecular weight of polymer
- M_w : Weight average molecular weight of polymer
- k_a, k_d : Rate constants of activation and deactivation steps of the initiation in radical polymerization
- k_i, k_p, k_t : Rate constants of initiation, propagation and termination steps in radical polymerization

KINETIC EFFECT OF ALKYLATED LINEAR AMINE LIGANDS IN HOMOGENOUS ATOM TRANSFER RADICAL POLYMERIZATION

SUMMARY

Atom transfer radical polymerization (ATRP) has become one of the most efficient and widely used controlled radical polymerization method to obtain polymers and copolymers with different topologies.

Transition metal catalysts are the key to ATRP since they determine the position of the atom transfer equilibrium and the dynamics of exchange between the dormant and active species. The main effect of the ligand is to solubilize the transition-metal salt in organic media and to regulate the proper reactivity and dynamic halogen exchange between the metal center and the dormant species or persistent radical. Ligands, typically amines or phosphines, are used to increase the solubility of the complex transition metal salts in the solution and to tune the reactivity of the metal towards halogen abstraction.

In this study, alkylated tridentate and tetradentate novel linear nitrogen ligands was used in ATRP of styrene (St) and methyl methacrylate (MMA) which was carried out in the presence of CuBr as co-catalyst and ethyl-2-bromo propionate (for St) and ethyl-2-bromo isobutyrate (for MMA) as initiator. The kinetic effect of those different ligands was examined on controlled radical polymerization.

ALKİLENMİŞ LİNEER AMİN LİGANDLARIN HOMOJEN ATOM TRANSFER RADİKAL POLİMERİZASYONUNA KİNETİK ETKİLERİ

ÖZET

Atom transfer radikal polimerizasyonu (ATRP), değişik topolojilerde polimerler ve kopolimerler elde etmekte kullanılan etkin ve çok kullanılan kontrollü radikal polimerizasyon metodu haline gelmiştir.

Geçiş metali katalizleri, deaktif ve aktif parçacıklar arasında atom transfer dengesi ile değişim dinamiğini belirlediği için ATRP de anahtar rolü görürler. Ligandın yerine getirdiği asıl görev geçiş metali tuzunu organik ortamda çözünür hale getirmek, uygun reaktiviteyi ve deaktif, aktif merkezler ile metal merkez arasındaki halojen değişimini regüle etmektir. Genellikler aminler ve fosfinler geçiş metal tuzunun çözültideki çözünürlüğünü arttırmak ve metalin halojen tutma reaktivitesini ayarlamak için ligand olarak kullanılırlar.

Bu çalışmada, alkillenmiş üç dişli ve dört dişli yeni lineer azot ligandları ile stiren (St) ve metil metakrilat (MMA) monomerlerinin, ko-katalizör CuBr varlığında, etil-2-bromo propiyonat (St için) ve etil-2-bromo izobutirat (MMA için) başlatıcıları ile atom transfer radikal polimerizasyonları gerçekleştirilmiştir. Bu değişik ligandların kontrollü radikal polimerizasyon üzerindeki kinetik etkileri incelenmiştir.

1. INTRODUCTION

Metal mediated radical polymerization, more generally known as atom transfer radical polymerization (ATRP), has become one of the most efficient controlled/living radical polymerization methods to obtain linear polymers and copolymers with different topologies. The catalyst–ligand complex in ATRP plays a key role in controlling the chain growth, polymerization rate, and polydispersity. The main effect of the ligand is to solubilize the transition-metal salt in the organic media and to regulate the proper reactivity and dynamic halogen exchange between the metal center and the dormant species or persistent radical [1].

Ligands, typically amines or phosphines, are used to increase the solubility of the transition metal salts in the solution and to tune the reactivity of the metal towards halogen abstraction. Tridentate and tetradentate ligands generally provide faster polymerizations than bidentate ligands, while monodentate nitrogen ligands yield redox-initiated free radical polymerization. In addition, ligands with an ethylene linkage between the nitrogens are more efficient than those with a propylene or butylene linkage.

Solubility of the ligand and its Cu(I) and Cu(II) complexes in organic media is of particular importance to attain homogeneous polymerization conditions. The ligand with a long aliphatic chain on the nitrogen atoms provides solubility of its metal complexes in organic solvents [2]. However, the increasing length of the alkyl substituents induces steric effects and can alter the redox potential of the metal center. Any shift in the redox potential affects the electron transfer and the activation– deactivation equilibrium [3].

In this study, alkylated tridentate and tetradentate novel linear amine ligands was used in ATRP of styrene (St) and methyl methacrylate (MMA) which was carried out in the presence of CuBr as co-catalyst and ethyl-2-bromo propionate (for St) and

ethyl-2-bromo isobutyrate (for MMA) as initiator. The kinetic effect of those different ligands was examined on controlled radical polymerization.

2. THEORETICAL PART

2.1. Conventional Free Radical Polymerizations

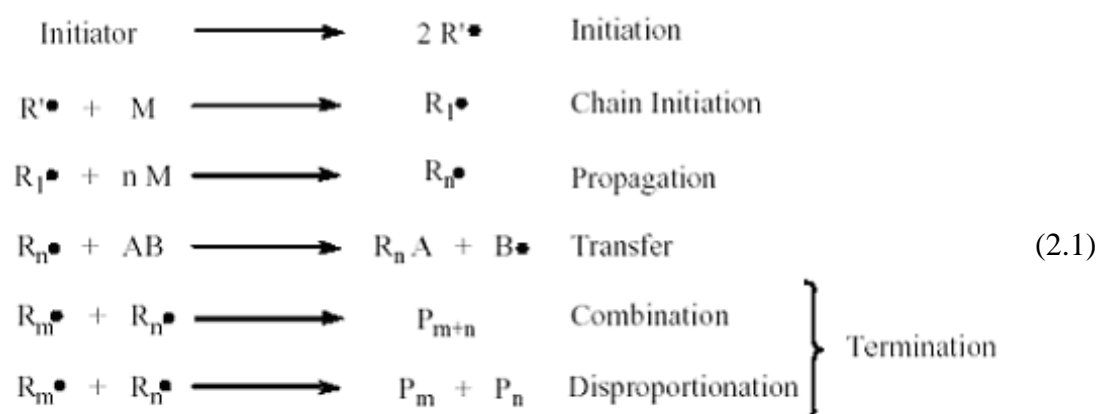
Free radical polymerizations are of significant importance in the industrial sector for a variety of reasons. First, many monomers capable of undergoing chain reactions are available in large quantities from the petrochemical sector [4]. In addition, free radical mechanisms are well understood and extension of the concepts to new monomers is generally straightforward. A third advantage of free radical routes is that the polymerization proceeds in a relatively facile manner: rigorous removal of moisture is generally unnecessary while polymerization can be carried out in either the bulk phase or in solution. As chain reactions, free radical polymerizations proceed via four distinct processes:

1. *Initiation*. In this first step, a reactive site is formed, thereby “initiating” the polymerization.
2. *Propagation*. Once an initiator activates the polymerization, monomer molecules are added one by one to the active chain end in the propagation step. The reactive site is regenerated after each addition of monomer.
3. *Transfer*: occurs when an active site is transferred to an independent molecule such as monomer, initiator, polymer, or solvent. This process results in both a terminated molecule (see step four) and a new active site that is capable of undergoing propagation.
4. *Termination*. In this final step, eradication of active sites leads to “terminated,” or inert, macromolecules. Termination occurs via coupling reactions of two active centers (referred to as combination), or atomic transfer between active chains (termed disproportionation).

The free radical chain process is demonstrated schematically below (2.1): $R\cdot$ represents a free radical capable of initiating propagation; M denotes a molecule of monomer; R_m and R_n refer to propagating radical chains with degrees of

polymerization of m and n , respectively; AB is a chain transfer agent; and $P_n + P_m$ represent terminated macromolecules.

Because chain transfer may occur for every radical at any and all degrees of polymerization, the influence of chain transfer on the average degree of polymerization and on polydispersity carries enormous consequences. Furthermore, propagation is a first order reaction while termination is second order. Thus, the proportion of termination to propagation increases substantially with increasing free radical concentrations. Chain transfer and termination are impossible to control in classical free radical processes, a major downfall when control over polymerization is desired.



2.2. Controlled/"Living" Radical Polymerization

The term controlled/"living" radical polymerization (C/LRP) was initially used to describe a chain polymerization in which chain breaking reactions were absent [5,6]. In such an ideal system, after initiation is completed, chains only propagate and do not undergo transfer and termination. However, transfer and termination often occur in real system. Thus, living polymerization (LP, no chain breaking reactions) and controlled polymerization (CP, formation of well defined polymers) are two separate terms.

A controlled polymerization can be defined as a synthetic method for preparing polymers with predetermined molecular weights, low polydispersity and controlled functionality.

Transfer and termination are allowed in a controlled polymerization if their contribution is sufficiently reduced by the proper choice of the reaction conditions such that polymer structure is not affected. On the other hand, living polymerizations will lead to well defined polymers only if the following additional prerequisites are fulfilled:

- initiation is fast in comparison with propagation
- exchange between species of different reactivities is fast in comparison with propagation
- the rate of depropagation is low in comparison with propagation and the system is sufficiently homogeneous, in the sense of availability of active centers and mixing.

Well defined polymers [1] may be formed in radical polymerization only if chains are relatively short and concentration of active center (free radicals) is low enough. There is an apparent contradiction between these two requirements because usually a decrease of the concentration of radicals leads to higher molecular weights.

However, the two conditions can be accommodated in systems with reversible deactivation of growing radicals. The controlled polymerization requires a low proportion of deactivated chains, which can be achieved by keeping molecular weight sufficiently low. This necessitates a relatively high concentration of the initiator, or in other words, low $[M]_0 / [I]_0$ ratios. However, when $[I]_0$ is high, since the termination is bimolecular, contribution of termination becomes more significant when a large concentration of radicals $[R^\bullet]$ is generated.

Therefore establishing an exchange between dormant and active species is necessary to solve this discrepancy. The concentration of dormant species can be equal to $[I]_0$, and the concentration of momentarily active species to $[R^\bullet]$. The total number of growing chains will be equal to $[I]_0$, and radicals would be present at a very low stationary concentration, $[R^\bullet]$, and therefore the contribution of termination should be very low.

The three approaches have been used to control radical systems. The best examples of the first approach include stable free radical polymerization (SFRP), atom transfer radical polymerization (ATRP), and reversible addition-fragmentation transfer polymerization (RAFT) based on photolabile iniferters. The second approach is less common and may include some organometallic species such as Cr(III) or Al

One of the most important parameters in ATRP is the dynamics of exchange, especially the relative rate of deactivation. If the deactivation process is slow in comparison with propagation, then a classic redox initiation process operates leading to conventional, and not controlled, radical polymerization. Polydispersities in ATRP decrease with conversion, with the rate constant of deactivation, k_d , and also with the concentration of deactivator, $[X-M_t^{n+1}]$. They, however, increase with the propagation rate constant, k_p , and the concentration of initiator, $[R-X]_0$. This means that more uniform polymers are obtained at higher conversion, when the concentration of deactivator in solution is high and the concentration of initiator is low. Also, more uniform polymers are formed when deactivator is very reactive and monomer propagates slowly (styrene rather than acrylate) [22].

2.2.1.1. Monomers

A variety of monomers have been successfully polymerized using ATRP. Typical monomers include styrenes, (meth)acrylates, (meth)acrylamides, and acrylonitrile, which contain substituents that can stabilize the propagating radicals. Even under the same conditions using the same catalyst, each monomer has its own unique atom transfer equilibrium constant for its active and dormant species. In the absence of any side reactions other than radical termination by coupling or disproportionation, the magnitude of the equilibrium constant ($K_{eq}=k_a/k_d$) determines the polymerization rate.

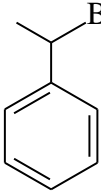
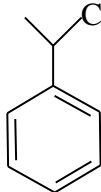
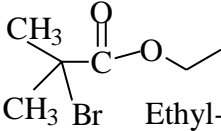
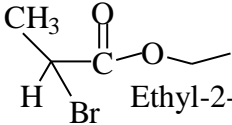
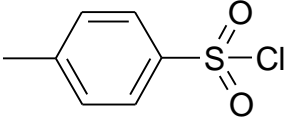
2.2.1.2. Initiators

The main role of the initiator is to determine the number of growing polymer chains. Two parameters are important for a successful ATRP initiating system. First, initiation should be fast in comparison with propagation. Second, the probability of the side reactions should be minimized.

In ATRP, alkyl halides (R-X) are typically used as initiator (Table 2.1.) and the rate of polymerization is first order with respect to the concentration of R-X. To obtain well-defined polymers with narrow molecular weight distributions, the halide group, X, must rapidly and selectively migrate between the growing chain and the transition metal complex. When X is either bromine or chlorine, the molecular weight control

is the best. Fluorine is not used because the C-F bond is too strong to undergo homolytic cleavage.

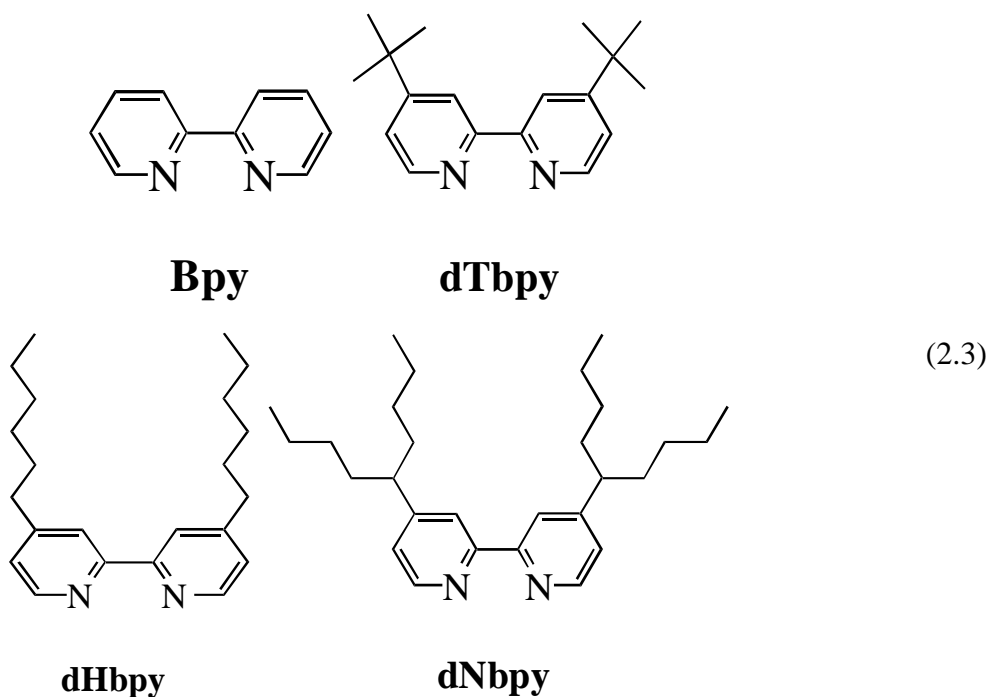
Table 2.1. The most frequently used initiator types in ATRP systems

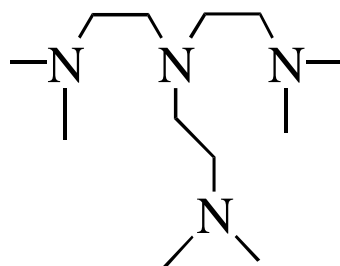
Initiator	Monomer
 1-Bromo-1-phenyl ethane	Styrene
 1-Chloro-1-phenyl ethane	Styrene
 Ethyl-2-bromo isobutyrate	Methyl methacrylate
 Ethyl-2-bromo propionate	Methyl acrylate and Styrene
 p-toluene sulphonyl chloride	Methyl methacrylate

2.2.1.3. Ligands

Transition metal catalysts are the key to ATRP since they determine the position of the atom transfer equilibrium and the dynamics of exchange between the dormant and active species. The main effect of the ligand is to solubilize the transition-metal

salt in organic media and to regulate the proper reactivity and dynamic halogen exchange between the metal center and the dormant species or persistent radical. Ligands, typically amines or phosphines, are used to increase the solubility of the complex transition metal salts in the solution and to tune the reactivity of the metal towards halogen abstraction. So far, a range of multidentate neutral nitrogen ligands was developed as active and efficient complexing agents for copper-mediated ATRP, including, bipyridines [23-25] (2.3), terpyridines [26,27], phenantrolines[28], picolyl amines [27,29], pyridinemethinamines [30-34] and tri [23,27,35-37] or tetradentate aliphatic amines [38-41] including linear and branched amines (2.4). Tridentate and tetradentate ligands generally provide faster polymerizations than bidentate ligands, while monodentate nitrogen ligands yield redox-initiated free radical polymerization. In addition, ligands with an ethylene linkage between the nitrogens are more efficient than those with a propylene or butylene linkage [3].

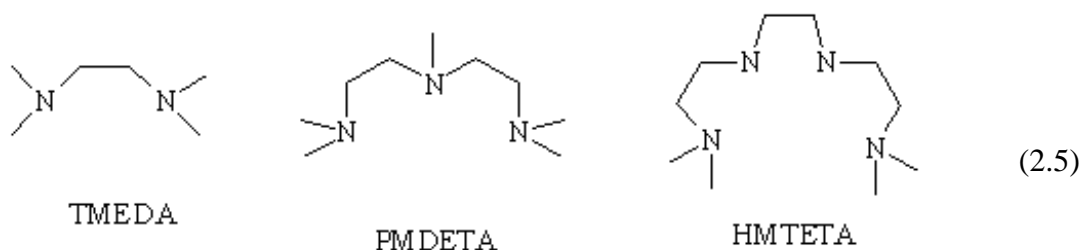




(2.4)

Me₆TREN

Linear amines with ethylene linkage like tetramethylethylenediamine (TMEDA), 1,1,4,7,7-pentamethyldiethylenetriamine (PMDETA), and 1,1,4,7,10,10-hexamethyltriethylenetetramine (HMTETA) (2.5) were synthesized and examined for ATRP as ligands [23]. Reasons for examining of these type of ligands are, they have low price, due to the absence of the extensive π -bonding in the simple amines, the subsequent copper complexes are less colored and since the coordination complexes between copper and simple amines tend to have lower redox potentials than the copper-bpy complex, the employment of simple amines as the ligand in ATRP may lead to faster polymerization rates.



(2.5)

Solubility of the ligand and its metal complexes in organic media is of particular importance to attain homogeneous polymerization conditions. The rate of polymerization is also affected by the relative solubilities of the activating and the deactivating species of the catalyst. In heterogeneous systems, a low stationary concentration of the catalyst species allows for a controlled polymerization, but the polymerization is much slower than in homogeneous systems [3]. The ligand with a long aliphatic chain on the nitrogen atoms provides solubility of its metal complexes

in organic solvents. However, the increasing length of the alkyl substituents induces steric effects and can alter the redox potential of the metal center. Any shift in the redox potential affects the electron transfer and the activation–deactivation equilibrium [27].

2.2.1.4. Transition Metal Complexes

Catalyst is the most important component of ATRP. It is the key to ATRP since it determines the position of the atom transfer equilibrium and the dynamics of exchange between the dormant and active species. There are several prerequisites for an efficient transition metal catalyst. First, the metal center must have at least two readily accessible oxidation states separated by one electron. Second the metal center should have reasonable affinity toward a halogen. Third the coordination sphere around the metal should be expandable upon oxidation to selectively accommodate a (pseudo)-halogen. Fourth the ligand should complex the metal relatively strong.

The most important catalysts used in ATRP are; Cu(I)Cl, Cu(I)Br, NiBr₂(PPh₃)₂, FeCl₂(PPh₃)₂, RuCl₂(PPh₃)₃/ Al(OR)₃.

2.2.1.5. Solvents

ATRP can be carried out either in bulk, in solution or in a heterogeneous system (e.g., emulsion, suspension). Various solvents such as benzene, toluene, anisole, diphenyl ether, ethyl acetate, acetone, dimethyl formamide (DMF), ethylene carbonate, alcohol, water, carbon dioxide and many others have been used for different monomers. A solvent is sometimes necessary especially when the obtained polymer is insoluble in its monomer.

2.2.1.6. Kinetics of ATRP

The rate of polymerization is first order with respect to monomer, alkyl halide (initiator), and transition metal complexed by ligand. The reaction is usually negative first order with respect to the deactivator ($X-M_t^{n+1}/Ligand$).

The rate equation of copper-based ATRP is formulated in discussed conditions and given in (2.6).

$$R_p = k_{app} [M] = k_p [R\cdot] [M] = k_p K_{eq} [I] ([CuX]/[CuX_2]) [M] \quad (2.6)$$

Figure 2.1 shows a typical linear variation of conversion with time in semi logarithmic coordinates (kinetic plot). Such a behavior indicates that there is a constant concentration of active species in the polymerization and first-order kinetics with respect to monomer. However, since termination occurs continuously, the concentration of the Cu(II) species increases and deviation from linearity may be observed [1]. For the ideal case with chain length independent from termination, persistent radical effect [42,43] kinetics implies the semi logarithmic plot of monomer conversion vs. time to the 2/3 exponent should be linear. Nevertheless, a linear semi logarithmic plot is often observed. This may be due to an excess of the Cu(II) species present initially, a chain length dependent termination rate coefficient, and heterogeneity of the reaction system due to limited solubility of the copper complexes. It is also possible that self-initiation may continuously produce radicals and compensate for termination. Similarly, external orders with respect to initiator and the Cu(I) species may also be affected by the persistent radical effect [44].

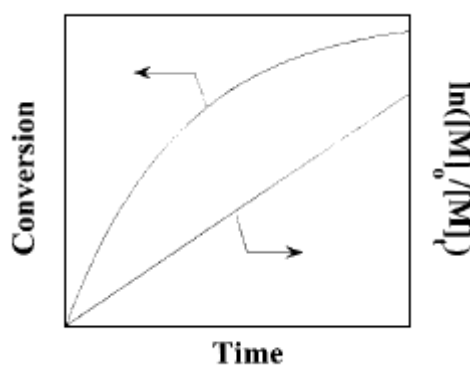


Figure 2.1 Kinetic plot and conversion vs. time plot for ATRP

Results from kinetic studies of ATRP for styrene (St) [45], methyl acrylate (MA) [46] and methyl methacrylate (MMA) [25,47] under homogeneous conditions indicate that the rate of polymerization is first order with respect to monomer,

initiator, and Cu(I) complex concentrations. These observations are all consistent with the derived rate law.

It should be noted that the optimum ratio can vary with regard to changes in the monomer, counter ion, ligand, temperature, and other factors [25,48,49]. The precise kinetic law for the deactivator CuX_2 was more complex due to the spontaneous generation of Cu(II) via the persistent radical effect [42,44,45]. In the atom transfer step, a reactive organic radical is generated along with a stable Cu(II) species that can be regarded as a persistent metallo-radical. If the initial concentration of deactivator Cu(II) in the polymerization is not sufficiently large to ensure a fast rate of deactivation ($k_d[\text{Cu(II)}]$), then coupling of the organic radicals will occur, leading to an increase in the Cu(II) concentration.

Radical termination occurs rapidly until a sufficient amount of deactivator Cu(II) is formed and the radical concentration is low. Under such conditions, the rate at which radicals combine (k_t) will become much slower than the rate at which radicals react with the Cu(II) complex in a deactivation process and a controlled polymerization will proceed. Typically, a small fraction (~5 %) of the total growing polymer chains will be terminated during the early stage of the polymerization, but the majority of the chains (>95 %) will continue to grow successfully. The effect of Cu(II) on the polymerization may additionally be complicated by its poor solubility, by a slow reduction by reaction with monomers leading to 1,2-dihaloadducts, or from the self-initiated systems such as styrene and other monomers.

If the deactivation does not occur, or if it is too slow ($k_p \gg k_d$), there will be no control and polymerization will become classical redox reaction therefore the termination and transfer reactions may be observed. To control the polymerization better, addition of one or a few monomers to the growing chain in each activation step is desirable. Molecular weight distribution for ATRP is given in (2.7).

$$M_w/M_n = 1 + ((k_d[\text{RX}]_0)/(k_p[\text{X-M}_t^{n+1}])) \times ((2/p)-1)$$

p = polymerization yield

$[\text{RX}]_0$ = concentration of the functional polymer chain

$[\text{X-M}_t^{n+1}]$ = concentration of the deactivators

k_d = rate constant of deactivation

k_p = rate constant of activation

(2.7)

When a hundred percent of conversion is reached, in other words $p=1$, it can be concluded that;

- a) For the smaller polymer chains, higher polydispersities are expected to be obtained because the smaller chains include little activation-deactivation steps and also the chain length difference is higher for small polymer chains resulting in little control of the polymerization.
- b) For the higher ratios of k_p/k_d , higher polydispersities (molecular weight distributions) are usually obtained resulting in the little control of polymerization.
- c) Resulting molecular weight distribution decreases as the concentration of the deactivators increases.

3. EXPERIMENTAL PART

3.1. Chemicals

Copper(I)bromide (CuBr, 99.99 %), 1,1,4,7,7-pentamethyldiethylenetriamine (PMDETA, 99 %), bipyridine (bpy, 98 %), and dinonylbipyridine (dNbpy, 97 %) were purchased from the Aldrich Chemical Co. MMA (99 %), St (99 %), ethyl-2-bromoisobutyrate (EiBB, used for MMA, 98 %), ethyl-2-bromopropionate (EBP, used for St, 99 %) were purchased from Acros Organics Co. Tris(2-(dimethylamino)-ethyl)amine (Me₆-TREN) [50], 1,1,4,7,7-pentaethyldiethylenetriamine (PEDETA), 1,1,4,7,7-pentabutyldiethylenetriamine (PBDETA), 1,1,4,7,7-pentahexyldiethylene triamine (PHDETA), 1,1,4,7,10,10-hexaethyltriethylenetetramine (HETETA), 1,1,4,7,10,10-hexabutyltriethylenetetramine (HBTETA) [51], 1,1,4,7,10,10-hexahexyltriethylenetetramine (HHTETA) [2] were synthesized according to modified literature procedure. All reagents were used without further purification.

3.2. Polymerization of Styrene

A typical ATRP procedure was performed as follows. Catalyst, CuBr (0,44 mmol) was placed in a 48 ml of flask, which contained a side arm with a Teflon valve sealed with a Teflon stopper. Then the flask was deoxygenated by vacuum-traw-nitrogen circles three times. St (7,93 mol l⁻¹) in anisole (10 % V/V) and ligand (0,0397 mol l⁻¹) (1,1,4,7,7-pentaethyldiethylenetriamine (PEDETA), 1,1,4,7,7-pentabutyldiethylene triamine (PBDETA), 1,1,4,7,7-pentahexyldiethylenetriamine (PHDETA), 1,1,4,7,10,10-hexaethyltriethylenetetramine (HETETA), 1,1,4,7,10,10-hexabutyl triethylenetetramine (HBTETA), 1,1,4,7,10,10-hexahexyltriethylenetetramine (HHTETA), 1,1,4,7,7-pentamethyldiethylenetriamine (PMDETA), bipyridine (bpy), dinonylbipyridine (dNbpy), tris(2-(dimethylamino)-ethyl)amine (Me₆-TREN)) were added to the flask. Finally, initiator ethyl-2-bromopropionate (EBP, 0,0397 mol l⁻¹) was added then the flask was replaced in thermostatically controlled oil bath at 110 °C. All liquid components were nitrogen bubbled prior to placement into the flask.

Monomer/initiator/catalyst/ligand ratio was 200/1/1/1 for St polymerizations. Samples were taken periodically via a syringe to follow the kinetics of the polymerization process. The samples were diluted with THF and methanol was added. GC and GPC measurements were performed.

3.3. Polymerization of Methyl Methacrylate

A typical ATRP procedure was performed as follows. Catalyst, CuBr (0,46 mmol,) was placed in a 48 ml of flask, which contained a side arm with a Teflon valve sealed with a Teflon stopper. Then the flask was deoxygenated by vacuum-traw-nitrogen circles three times. MMA (6,24 mol l⁻¹) in anisole (50 % V/V) and ligand (0,0312 mol l⁻¹) (1,1,4,7,7-pentaethyldiethylenetriamine (PEDETA), 1,1,4,7,7-pentabutyl diethylenetriamine (PBDETA), 1,1,4,7,7-pentahexyldiethylenetriamine (PHDETA), 1,1,4,7,10,10-hexaethyltriethylenetetramine (HETETA), 1,1,4,7,10,10-hexabutyl triethylenetetramine (HBTETA), 1,1,4,7,10,10-hexahexyltriethylenetetramine (HHTETA), 1,1,4,7,7-pentamethyldiethylenetriamine (PMDETA), bipyridine (bpy), dinonylbipyridine (dNbpy), tris(2-(dimethylamino)-ethyl)amine (Me₆-TREN)) were added to the flask. Finally, initiator ethyl-2-bromoisobutyrate (EiBB, 0,0312 mol l⁻¹) was added then the flask was replaced in thermostatically controlled oil bath at 80 °C. All liquid components were nitrogen bubbled prior to placement into the flask. Monomer/initiator/catalyst/ligand ratio was 200/1/1/1 for MMA polymerizations. Samples were taken periodically via a syringe to follow the kinetics of the polymerization process. The samples were diluted with THF and methanol was added. GC and GPC measurements were performed.

3.4. Characterization

Monomer conversion was determined by ATI Unicam gas chromatography (GC) equipped with a FID detector and a J&W scientific 15 m DB WAX widebore capillary column. Molecular weight and molecular weight distributions of polymer were measured on a gel permeation chromatography (GPC) system consisting of an Agilent 1100 series pump, four Waters Styragel HR columns (5E, 4E, 3, 2) and an Agilent 1100 RI detector, with a THF flow rate 0.3 ml min⁻¹; poly(methyl methacrylate) and polystyrene were used as standards.

4. RESULTS AND DISCUSSIONS

4.1. ATRP of Styrene

ATRP of styrene was carried out with different ligands in identical conditions which. St (7,93 mol l⁻¹) in anisole (10 % V/V), ligand (0,0397 mol l⁻¹), CuBr (0,44 mmol), ethyl-2-bromopropionate (EBP, 0,0397 mol l⁻¹) were used in these ATRP reactions. Reaction temperatures were set to 110 °C. $[M]_o/[I]_o/[CuBr]_o/[ligand]_o = 200/1/1/1$.

4.1.1. Using 1,1,4,7,7-pentaethyldiethylenetriamine (PEDETA)

The semi-logarithmic kinetic plot ($\ln([M]_o/[M])$ versus time) of ATRP reaction of St is shown in Figure 4.1 A straight line is observed indicating that the kinetics is first order with respect to the monomer concentration and demonstrates that active center concentration is constant during the polymerization. This result explains that termination is absent or negligible. Apparent rate constant of St polymerization using PEDETA at 110 °C was calculated from the figure as $k_{app}=0,87 \times 10^{-4} \text{ s}^{-1}$.

Molecular weight of the polymer versus conversion plot was shown in Figure 4.2 linear relationship indicates that transfer reactions are absent or insignificant. Measured molecular weights of the polymer are found close to theoretical ones.

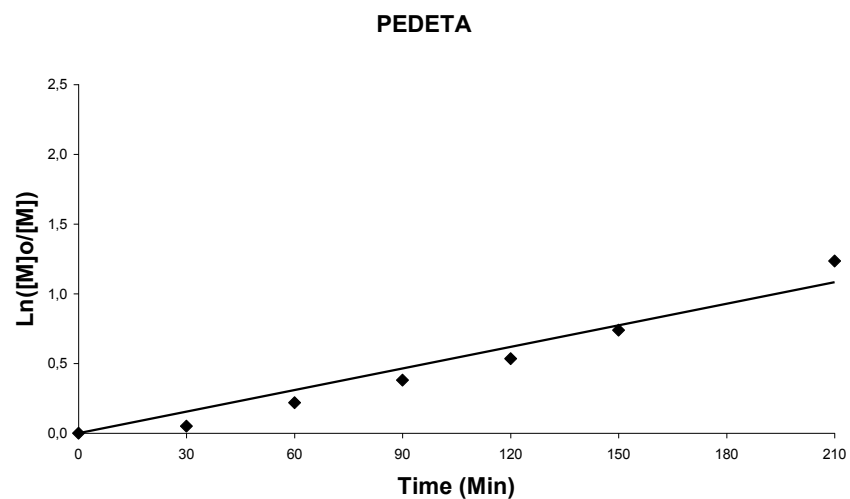


Figure 4.1 Semi-logarithmic kinetic plot for ATRP of St using PEDETA as a ligand. $[M]_0/[I]_0/[CuBr]_0/[PEDETA]_0=200/1/1/1$. $[St]=7,93 \text{ mol l}^{-1}$ in anisole (10 % V/V) at 110°C .

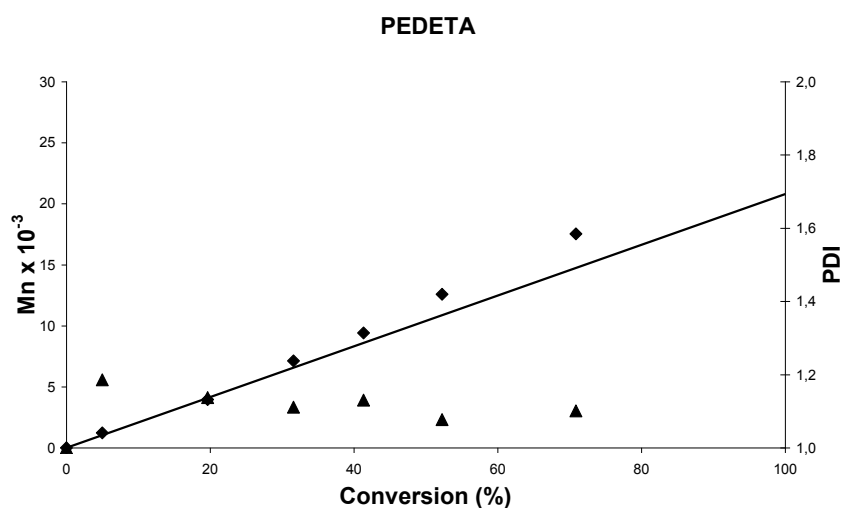


Figure 4.2 Molecular weight and molecular weight distribution versus conversion plot for ATRP of St using PEDETA (\blacklozenge : M_n , \blacktriangle : PDI). $[St]=7,93 \text{ mol l}^{-1}$ in anisole (10 % V/V) at 110°C . $[M]_0/[I]_0/[CuBr]_0/[PEDETA]_0=200/1/1/1$.

4.1.2. Using 1,1,4,7,7-pentabutyldiethylenetriamine (PBDETA)

The semi-logarithmic kinetic plot ($\ln([M]_0/[M])$ versus time) of ATRP reaction of St was shown in Figure 4.3 A straight line is observed indicating that the kinetics is first order with respect to the monomer concentration in the polymerization and demonstrates that active center concentration is constant during the polymerization. This result explains that termination is absent or negligible. Apparent rate constant of St polymerization using PBDETA at 110 °C was calculated from the figure as $k_{app}=0,58 \times 10^{-4} \text{ s}^{-1}$.

Molecular weight of the polymer versus conversion plot was shown in Figure 4.4 linear relationship indicates that transfer reactions are absent or insignificant. Measured molecular weights of the polymer are found close to theoretical ones.

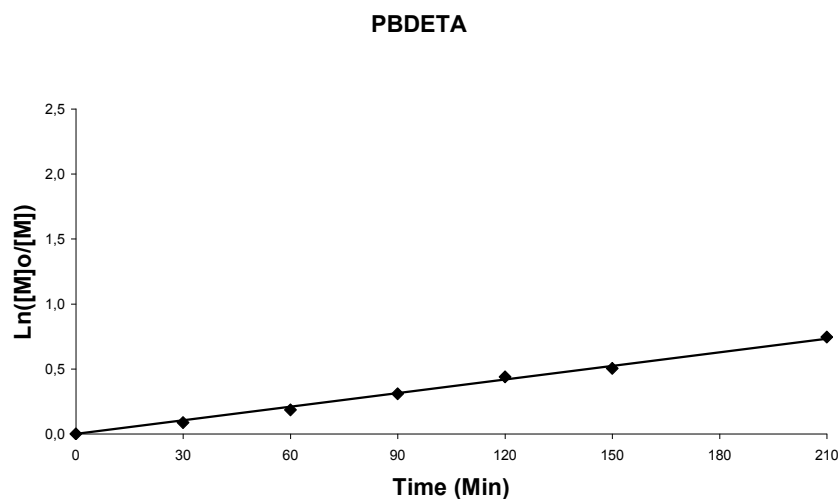


Figure 4.3 Semi-logarithmic kinetic plot for ATRP of St using PBDETA as a ligand. $[M]_0/[I]_0/[CuBr]_0/[PBDETA]_0=200/1/1/1$. $[St]=7,93 \text{ mol l}^{-1}$ in anisole (10 % V/V) at 110°C.

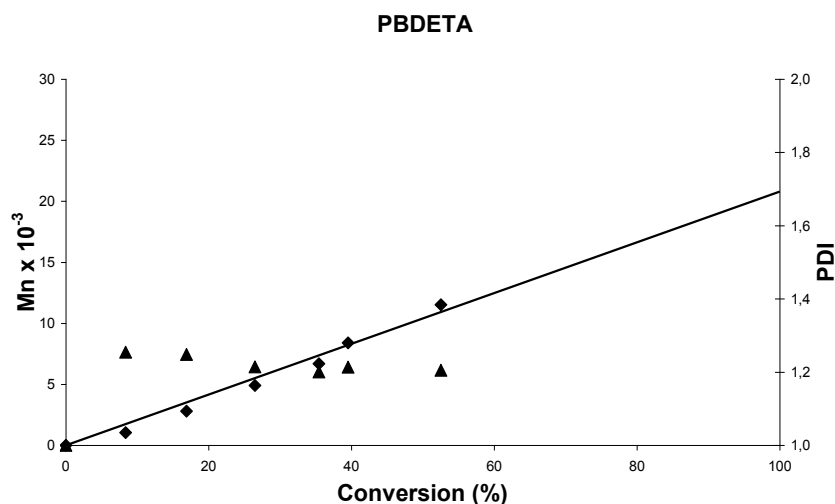


Figure 4.4 Molecular weight and molecular weight distribution versus conversion plot for ATRP of St using PBDETA (♦: Mn, ▲: PDI). $[St]=7,93 \text{ mol l}^{-1}$ in anisole (10 % V/V) at 110°C . $[M]_0/[I]_0/[CuBr]_0/[PBDETA]_0=200/1/1/1$.

4.1.3. Using 1,1,4,7,7-pentahexyldiethylenetriamine (PHDETA)

The semi-logarithmic kinetic plot ($\ln([M]_0/[M])$ versus time) of ATRP reaction of St was shown in Figure 4.5 A straight line is observed indicating that the kinetics is first order with respect to the monomer concentration in the polymerization and demonstrates that active center concentration is constant during the polymerization. This result explains that termination is absent or negligible. Apparent rate constant of St polymerization using PHDETA at 110°C was calculated from the figure as $k_{app}=0,52 \times 10^{-4} \text{ s}^{-1}$.

Molecular weight of the polymer versus conversion plot was shown in Figure 4.6 linear relationship indicates that transfer reactions are absent or insignificant. Measured molecular weights of the polymer are found close to theoretical ones.

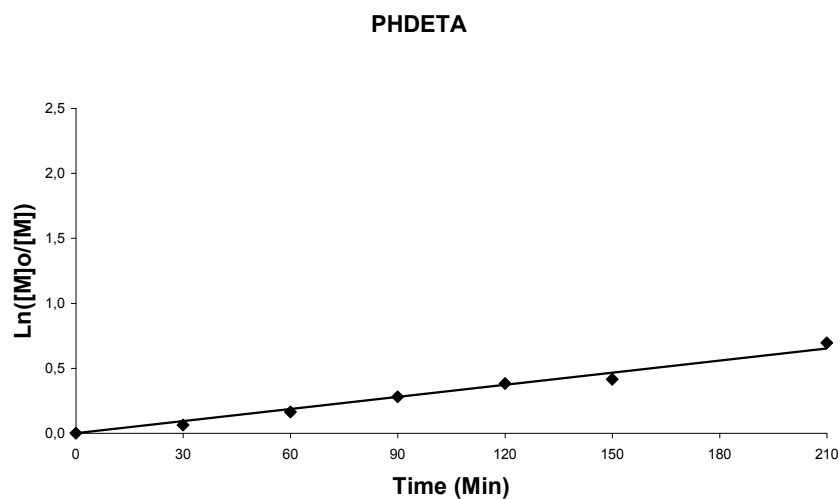


Figure 4.5 Semi-logarithmic kinetic plot for ATRP of St using PHDETA as a ligand. $[M]_0/[I]_0/[CuBr]_0/[PHDETA]_0=200/1/1/1$. $[St]=7,93 \text{ mol l}^{-1}$ in anisole (10 % V/V) at 110°C .

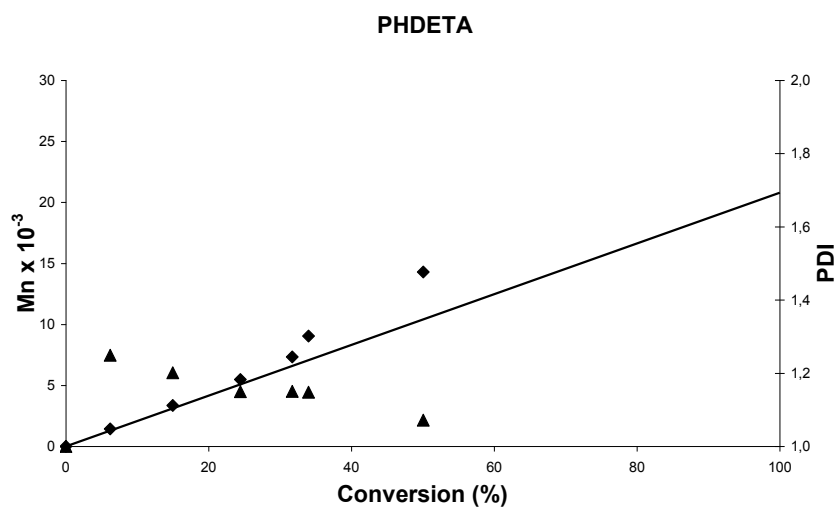


Figure 4.6 Molecular weight and molecular weight distribution versus conversion plot for ATRP of St using PHDETA (♦: Mn, ▲: PDI). $[St]=7,93 \text{ mol l}^{-1}$ in anisole (10 % V/V) at 110°C . $[M]_0/[I]_0/[CuBr]_0/[PHDETA]_0=200/1/1/1$.

4.1.4. Using 1,1,4,7,10,10-hexaethyltriethylenetetramine (HETETA)

The semi-logarithmic kinetic plot ($\ln([M]_0/[M])$ versus time) of ATRP reaction of St was shown in Figure 4.7 A straight line is observed indicating that the kinetics is first order with respect to the monomer concentration in the polymerization and demonstrates that active center concentration is constant during the polymerization. This result explains that termination is absent or negligible. Apparent rate constant of St polymerization using HETETA at 110 °C was calculated from the figure as $k_{app}=1,15 \times 10^{-4} \text{ s}^{-1}$.

Molecular weight of the polymer versus conversion plot was shown in Figure 4.8 linear relationship indicates that transfer reactions are absent or insignificant. Measured molecular weights of the polymer are found close to theoretical ones.

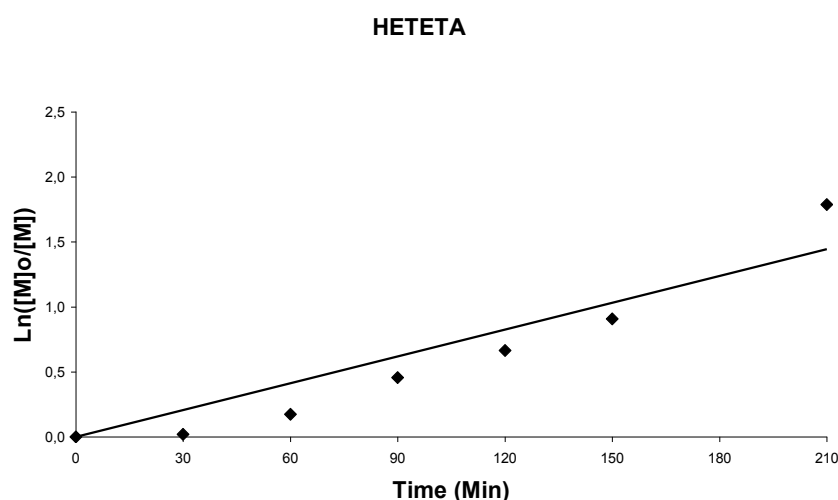


Figure 4.7 Semi-logarithmic kinetic plot for ATRP of St using HETETA as a ligand. $[M]_0/[I]_0/[CuBr]_0/[HETETA]_0=200/1/1/1$. $[St]=7,93 \text{ mol l}^{-1}$ in anisole (10 % V/V) at 110°C.

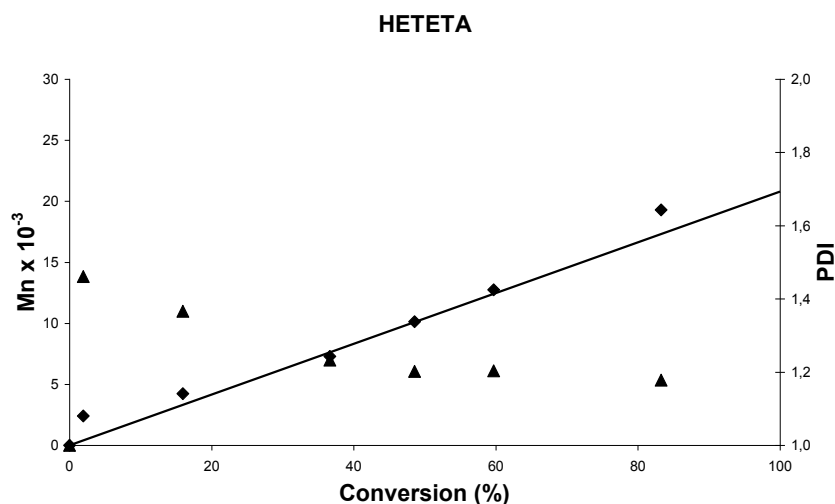


Figure 4.8 Molecular weight and molecular weight distribution versus conversion plot for ATRP of St using HETETA (♦: Mn, ▲: PDI). $[St]=7,93 \text{ mol l}^{-1}$ in anisole (10 % V/V) at 110°C . $[M]_0/[I]_0/[CuBr]_0/[HETETA]_0=200/1/1/1$.

4.1.5. Using 1,1,4,7,10,10-hexabutyltriethylenetetramine (HBTETA)

The semi-logarithmic kinetic plot ($\ln([M]_0/[M])$ versus time) of ATRP reaction of St was shown in Figure 4.9 A straight line is observed indicating that the kinetics is first order with respect to the monomer concentration in the polymerization and demonstrates that active center concentration is constant during the polymerization. This result explains that termination is absent or negligible. Apparent rate constant of St polymerization using HBTETA at 110°C was calculated from the figure as $k_{app}=0,87 \times 10^{-4} \text{ s}^{-1}$.

Molecular weight of the polymer versus conversion plot was shown in Figure 4.10 linear relationship indicates that transfer reactions are absent or insignificant. Measured molecular weights of the polymer are found close to theoretical ones.

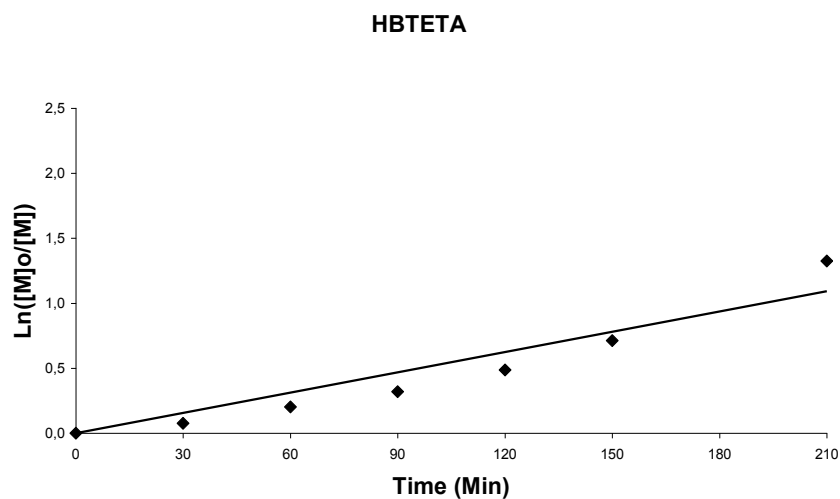


Figure 4.9 Semi-logarithmic kinetic plot for ATRP of St using HBTETA as a ligand. $[M]_0/[I]_0/[CuBr]_0/[HBTETA]_0=200/1/1/1$. $[St]=7,93 \text{ mol l}^{-1}$ in anisole (10 % V/V) at 110°C .

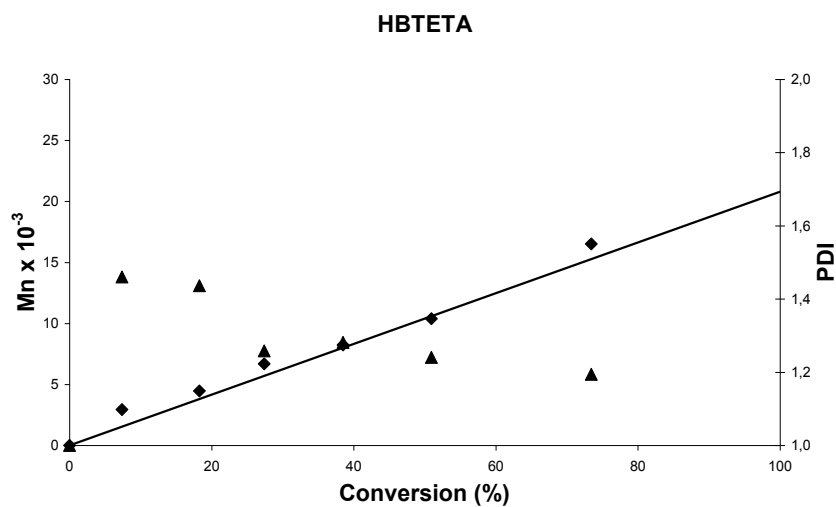


Figure 4.10 Molecular weight and molecular weight distribution versus conversion plot for ATRP of St using HBTETA (♦: M_n , ▲: PDI). $[St]=7,93 \text{ mol l}^{-1}$ in anisole (10 % V/V) at 110°C . $[M]_0/[I]_0/[CuBr]_0/[HBTETA]_0=200/1/1/1$.

4.1.6. Using 1,1,4,7,10,10-hexahexyltriethylenetetramine (HHTETA)

The semi-logarithmic kinetic plot ($\ln([M]_0/[M])$ versus time) of ATRP reaction of St was shown in Figure 4.11 A straight line is observed indicating that the kinetics is first order with respect to the monomer concentration in the polymerization and demonstrates that active center concentration is constant during the polymerization. This result explains that termination is absent or negligible. Apparent rate constant of St polymerization using HHTETA at 110 °C was calculated from the figure as $k_{app}=0,80 \times 10^{-4} \text{ s}^{-1}$.

Molecular weight of the polymer versus conversion plot was shown in Figure 4.12 linear relationship indicates that transfer reactions are absent or insignificant. Measured molecular weights of the polymer are found close to theoretical ones.

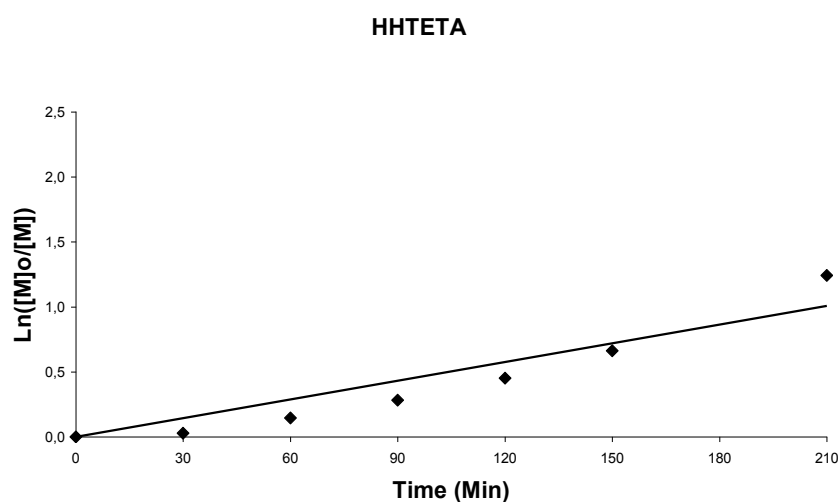


Figure 4.11 Semi-logarithmic kinetic plot for ATRP of St using HHTETA as a ligand. $[M]_0/[I]_0/[CuBr]_0/[HHTETA]_0=200/1/1/1$. $[St]=7,93 \text{ mol l}^{-1}$ in anisole (10 % V/V) at 110°C.

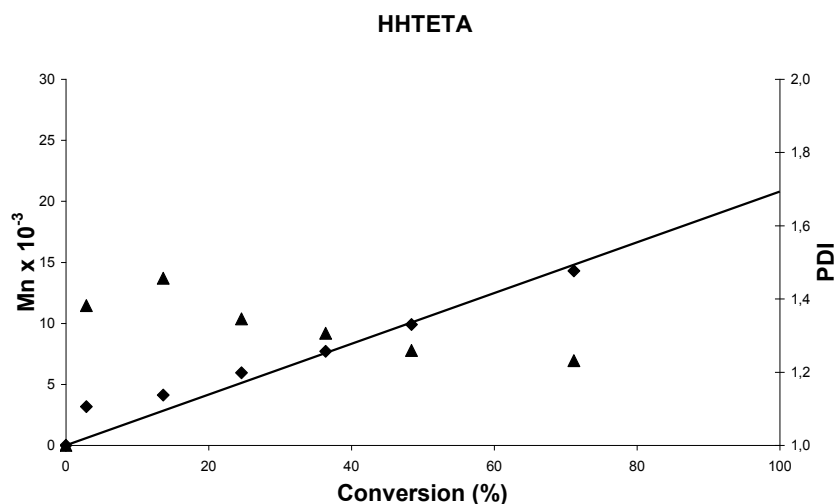


Figure 4.12 Molecular weight and molecular weight distribution versus conversion plot for ATRP of St using HHTETA (♦: Mn, ▲: PDI). $[St]=7,93 \text{ mol l}^{-1}$ in anisole (10 % V/V) at 110°C . $[M]_0/[I]_0/[CuBr]_0/[HHTETA]_0=200/1/1/1$.

4.1.7. Using 1,1,4,7,7-pentamethyldiethylenetriamine (PMDETA)

The semi-logarithmic kinetic plot ($\ln([M]_0/[M])$ versus time) of ATRP reaction of St was shown in Figure 4.13 A straight line is observed indicating that the kinetics is first order with respect to the monomer concentration in the polymerization and demonstrates that active center concentration is constant during the polymerization. This result explains that termination is absent or negligible. Apparent rate constant of St polymerization using PMDETA at 110°C was calculated from the figure as $k_{app}=0,78 \times 10^{-4} \text{ s}^{-1}$.

Molecular weight of the polymer versus conversion plot was shown in Figure 4.14 linear relationship indicates that transfer reactions are absent or insignificant. Measured molecular weights of the polymer are found close to theoretical ones.

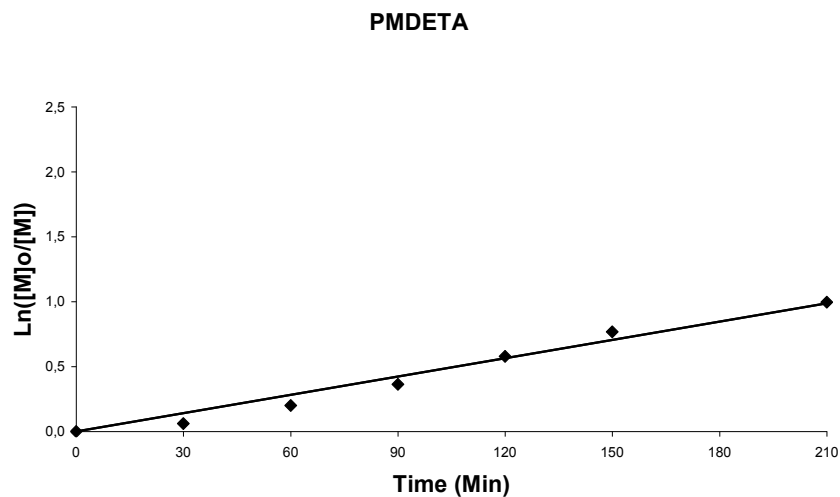


Figure 4.13 Semi-logarithmic kinetic plot for ATRP of St using PMDETA as a ligand. $[M]_0/[I]_0/[CuBr]_0/[PMDETA]_0=200/1/1/1$. $[St]=7,93 \text{ mol l}^{-1}$ in anisole (10 % V/V) at 110°C .

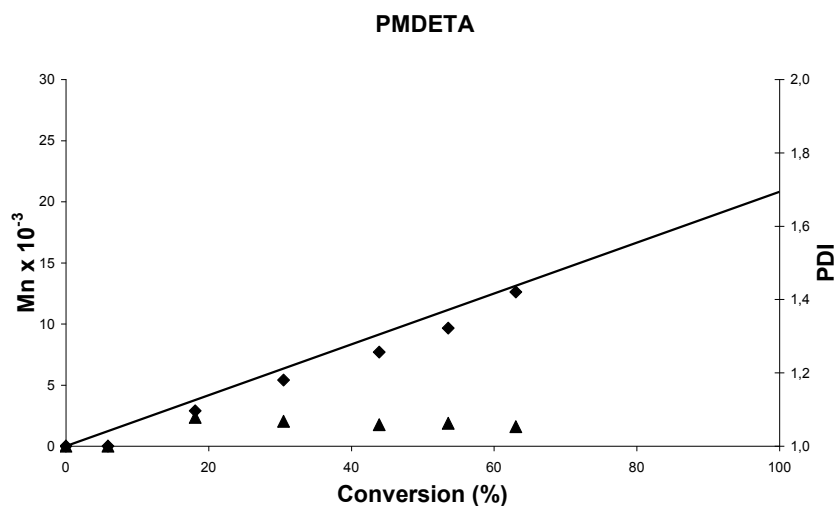


Figure 4.14 Molecular weight and molecular weight distribution versus conversion plot for ATRP of St using PMDETA (♦: Mn, ▲: PDI). $[St]=7,93 \text{ mol l}^{-1}$ in anisole (10 % V/V) at 110°C . $[M]_0/[I]_0/[CuBr]_0/[PMDETA]_0=200/1/1/1$.

4.1.8. Using bipyridine (bpy)

The semi-logarithmic kinetic plot ($\ln([M]_0/[M])$ versus time) of ATRP reaction of St was shown in Figure 4.15. A straight line is observed indicating that the kinetics is first order with respect to the monomer concentration in the polymerization and demonstrates that active center concentration is constant during the polymerization. This result explains that termination is absent or negligible. Apparent rate constant of St polymerization using bpy at 110 °C was calculated from the figure as $k_{app}=0,15 \times 10^{-4} \text{ s}^{-1}$.

Molecular weight of the polymer versus conversion plot was shown in Figure 4.16. A linear relationship indicates that transfer reactions are absent or insignificant. Measured molecular weights of the polymer are found close to theoretical ones.

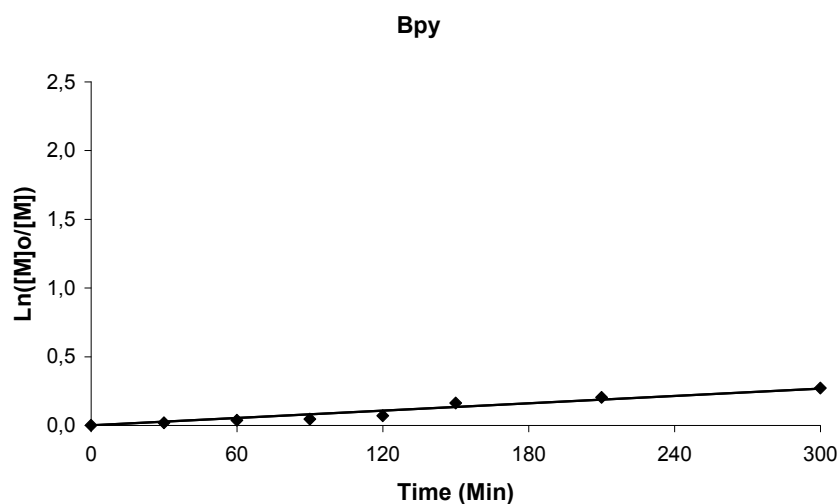


Figure 4.15 Semi-logarithmic kinetic plot for ATRP of St using bpy as a ligand. $[M]_0/[I]_0/[CuBr]_0/[bpy]_0=200/1/1/1$. $[St]=7,93 \text{ mol l}^{-1}$ in anisole (10 % V/V) at 110°C.

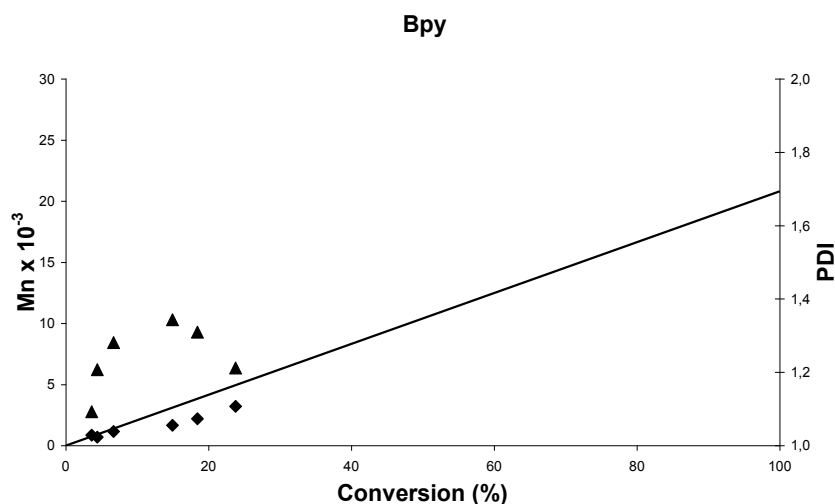


Figure 4.16 Molecular weight and molecular weight distribution versus conversion plot for ATRP of St using bpy (◆: Mn, ▲: PDI). $[St]=7,93 \text{ mol l}^{-1}$ in anisole (10 % V/V) at 110°C . $[M]_0/[I]_0/[CuBr]_0/[bpy]_0=200/1/1/1$.

4.1.9. Using dinonylbipyridine (dNbpy)

The semi-logarithmic kinetic plot ($\ln([M]_0/[M])$ versus time) of ATRP reaction of St was shown in Figure 4.17 A straight line is observed indicating that the kinetics is first order with respect to the monomer concentration in the polymerization and demonstrates that active center concentration is constant during the polymerization. This result explains that termination is absent or negligible. Apparent rate constant of St polymerization using dNbpy at 110°C was calculated from the figure as $k_{app}=0,12 \times 10^{-4} \text{ s}^{-1}$.

Molecular weight of the polymer versus conversion plot was shown in Figure 4.18 Linear relationship indicates that transfer reactions are absent or insignificant. Measured molecular weights of the polymer are found close to theoretical ones.

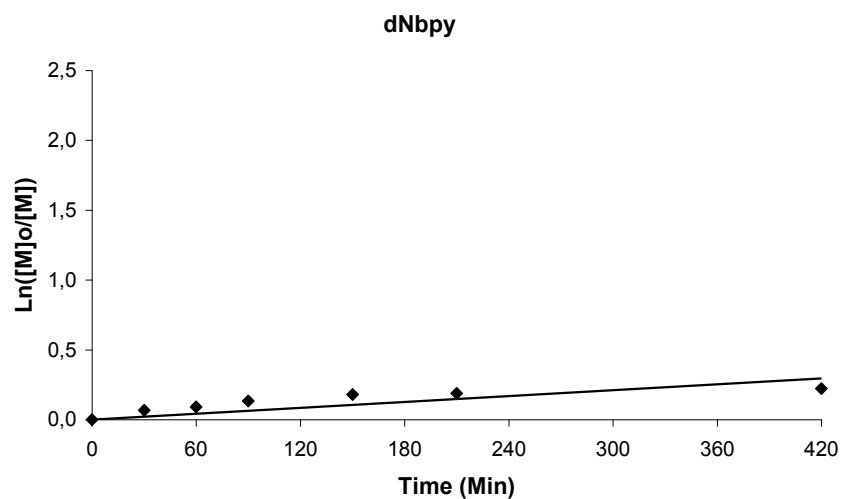


Figure 4.17 Semi-logarithmic kinetic plot for ATRP of St using dNbpy as a ligand. $[M]_0/[I]_0/[CuBr]_0/[dNbpy]_0=200/1/1/1$. $[St]=7,93 \text{ mol l}^{-1}$ in anisole (10 % V/V) at 110°C

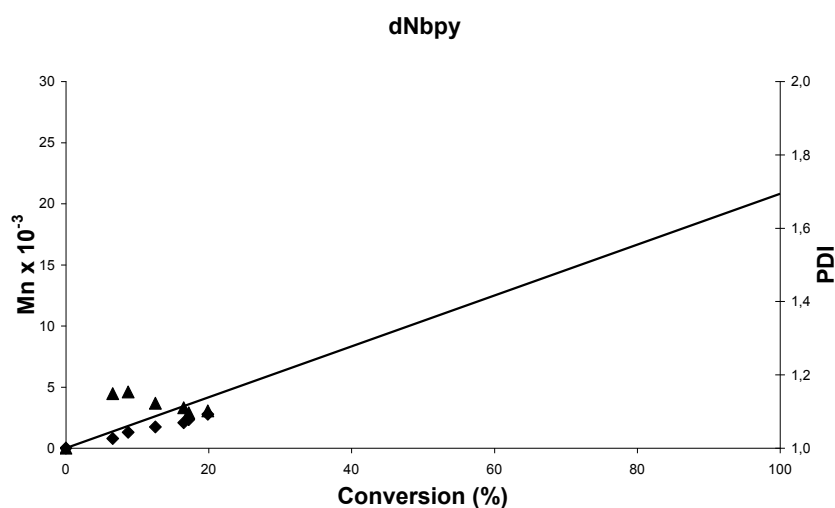


Figure 4.18 Molecular weight and molecular weight distribution versus conversion plot for ATRP of St using dNbpy (\blacklozenge : M_n , \blacktriangle : PDI). $[St]=7,93 \text{ mol l}^{-1}$ in anisole (10 % V/V) at 110°C . $[M]_0/[I]_0/[CuBr]_0/[dNbpy]_0=200/1/1/1$.

4.1.10. Using tris(2-(dimethylamino)-ethyl)amine (Me₆-TREN)

The semi-logarithmic kinetic plot ($\ln([M]_0/[M])$ versus time) of ATRP reaction of St was shown in Figure 4.19 A straight line is observed indicating that the kinetics is first order with respect to the monomer concentration in the polymerization and demonstrates that active center concentration is constant during the polymerization. This result explains that termination is absent or negligible. Apparent rate constant of St polymerization using Me₆-TREN at 110 °C was calculated from the figure as $k_{app}=0,78 \times 10^{-4} \text{ s}^{-1}$.

Molecular weight of the polymer versus conversion plot was shown in Figure 4.20 linear relationship indicates that transfer reactions are absent or insignificant. Measured molecular weights of the polymer are found close to theoretical ones.

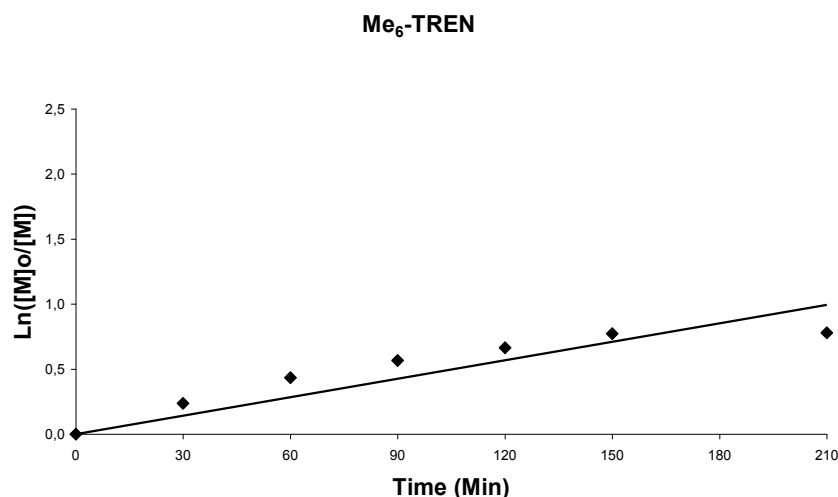


Figure 4.19 Semi-logarithmic kinetic plot for ATRP of St using Me₆-TREN as a ligand. $[M]_0/[I]_0/[CuBr]_0/[Me_6-TREN]_0=200/1/1/1$. $[St]=7,93 \text{ mol l}^{-1}$ in anisole (10 % V/V) at 110°C.

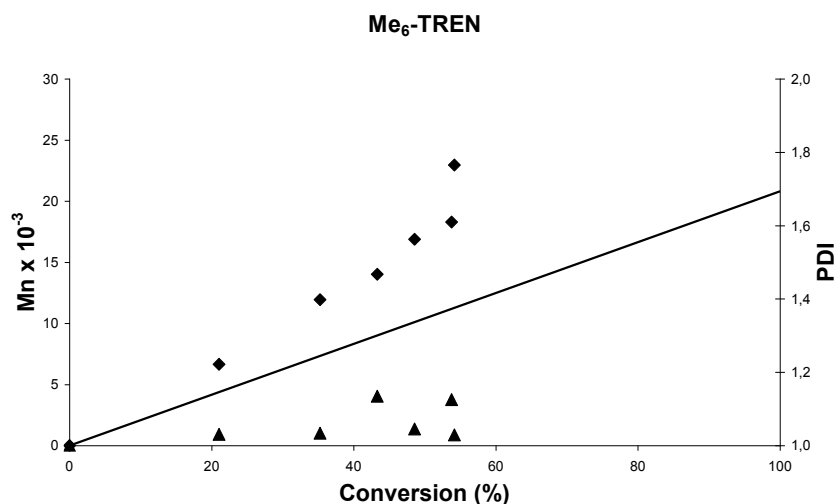


Figure 4.20 Molecular weight and molecular weight distribution versus conversion plot for ATRP of St using Me₆-TREN (◆: Mn, ▲: PDI). [St]=7,93 mol l⁻¹ in anisole (10 % V/V) at 110°C. [M]₀/[I]₀/[CuBr]₀/[Me₆-TREN]₀=200/1/1/1.

4.2. Results for ATRP of Styrene

Ten experiments performed for ATRP of St in conditions explained above. For each of the experiment;

- Rate of polymerization (R_p) calculated from semi-logarithmic kinetic plot,
- M_n and M_w of polymers measured by GPC method,
- Initiator efficiencies are calculated using theoretical M_n and measured M_n values,
- Polymers with low polydispersity index (PDI) are obtained.

Results collected from these ten experiments and results from a reference [2], are shown in Table 4.1.

Table 4.1. Results for ATRP of St in carried out experiments

Ligand	Time (min)	Conv * (%)	$M_{n,Cat}$	$M_{n,GPC}^*$	PDI*	R_p ($10^{-4} s^{-1}$)	Ini Eff. (f)
PEDETA^a	210	71	14800	17500	1,10	0,87	0,85
PBDETA^a	210	53	11050	11500	1,20	0,58	0,96
PHDETA^a	210	50	10400	14300	1,07	0,52	0,73
HETETA^a	210	83	17300	19300	1,17	1,15	0,90
HBTETA^a	210	73	15200	16500	1,19	0,87	0,92
HHTETA^a	210	71	14800	14300	1,23	0,80	1,00
PMDETA^a	210	63	13100	12600	1,05	0,78	1,00
bpy^a	300	24	5000	3200	1,21	0,15	>1,00
dNbpy^a	420	20	4150	2800	1,10	0,12	>1,00
Me₆TREN^a	210	54	11250	22900	1,03	0,78	0,49
HHTETA^{b,1}	120	74	15400	13000	1,15	1,70	1,00

^a [St]=7,93 mol l⁻¹ in anisole (10 % V/V) at 110 °C. [M]₀/[I]₀/[CuBr]₀/[ligand]₀=200/1/1/1

^b [St]=8,4 mol l⁻¹ (bulk) at 110 °C. [M]₀/[1-PEBr]₀/[CuBr]₀/[HHTETA]₀=200/1/1/1

¹ Ref. [2]

* Last point of kinetic data

In these ATRP reactions homogeneity has been achieved by using PEDETA, PBDETA, PHDETA, HETETA, HBTETA, HHTETA and dNbpy ligands. HETETA has the highest R_p for St in examined ligands. R_p has been decreased by increasing of the alkyl chain length for both linear tridentate and tetradentate linear amine ligands.

4.3. ATRP of Methyl Methacrylate

ATRP of MMA was carried out with different ligands in identical conditions which will be explained as follows. MMA ($6,24 \text{ mol l}^{-1}$) in anisole (50 % V/V), ligand ($0,0312 \text{ mol l}^{-1}$), CuBr ($0,46 \text{ mmol}$), ethyl-2-bromoisobutyrate (EiBB, $0,0312 \text{ mol l}^{-1}$) were used in these ATRP reactions. Reaction temperatures were set to $80 \text{ }^\circ\text{C}$. $[M]_0/[I]_0/[CuBr]_0/[ligand]_0 = 200/1/1/1$.

4.3.1. Using 1,1,4,7,7-pentaethyldiethylenetriamine (PEDETA)

The semi-logarithmic kinetic plot ($\ln([M]_0/[M])$ versus time) of ATRP reaction of MMA was shown in Figure 4.21 A straight line is observed indicating that the kinetics is first order with respect to the monomer concentration in the polymerization and demonstrates that active center concentration is constant during the polymerization. This result explains that termination is absent or negligible. Apparent rate constant of MMA polymerization using PEDETA at $80 \text{ }^\circ\text{C}$ was calculated from the figure as $k_{app}=3,30 \times 10^{-4} \text{ s}^{-1}$.

Molecular weight of the polymer versus conversion plot was shown in Figure 4.22 linear relationship indicates that transfer reactions are absent or insignificant. Measured molecular weights of the polymer are found close to theoretical ones.

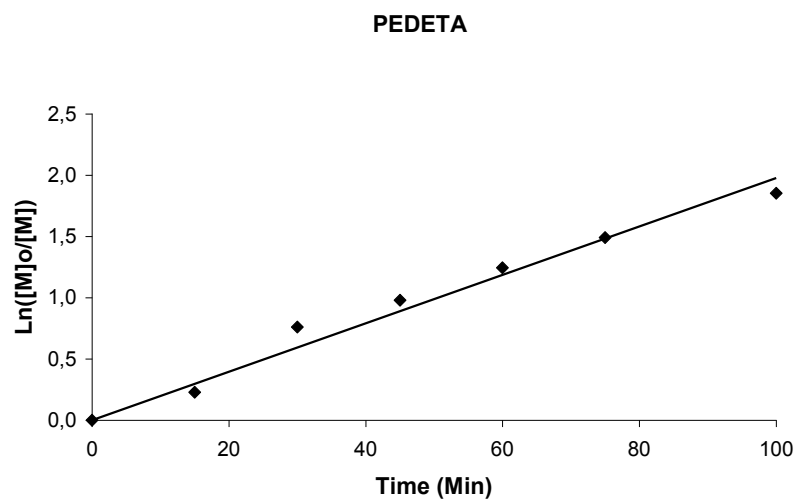


Figure 4.21 Semi-logarithmic kinetic plot for ATRP of MMA using PEDETA as a ligand. $[M]_0/[I]_0/[CuBr]_0/[PEDETA]_0=200/1/1/1$. $[MMA]=6,24 \text{ mol l}^{-1}$ in anisole (50 % V/V) at 80°C .

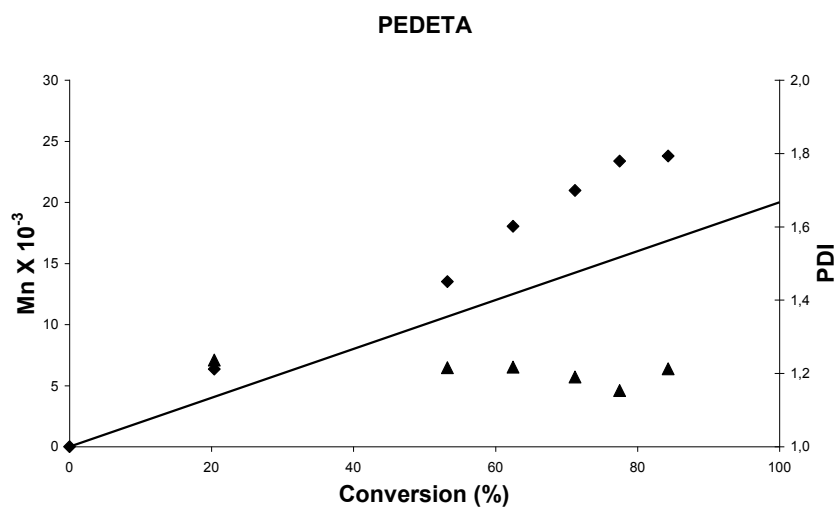


Figure 4.22 Molecular weight and molecular weight distribution versus conversion plot for ATRP of MMA using PEDETA (\blacklozenge : M_n , \blacktriangle : PDI). $[MMA]=6,24 \text{ mol l}^{-1}$ in anisole (50 % V/V) at 80°C . $[M]_0/[I]_0/[CuBr]_0/[PEDETA]_0=200/1/1/1$.

4.3.2. Using 1,1,4,7,7-pentabutyldiethylenetriamine (PBDETA)

The semi-logarithmic kinetic plot ($\ln([M]_0/[M])$ versus time) of ATRP reaction of MMA was shown in Figure 4.23 A straight line is observed indicating that the kinetics is first order with respect to the monomer concentration in the polymerization and demonstrates that active center concentration is constant during the polymerization. This result explains that termination is absent or negligible. Apparent rate constant of MMA polymerization using PBDETA at 80 °C was calculated from the figure as $k_{app}=2,85 \times 10^{-4} \text{ s}^{-1}$.

Molecular weight of the polymer versus conversion plot was shown in Figure 4.24 linear relationship indicates that transfer reactions are absent or insignificant. Measured molecular weights of the polymer are found close to theoretical ones.

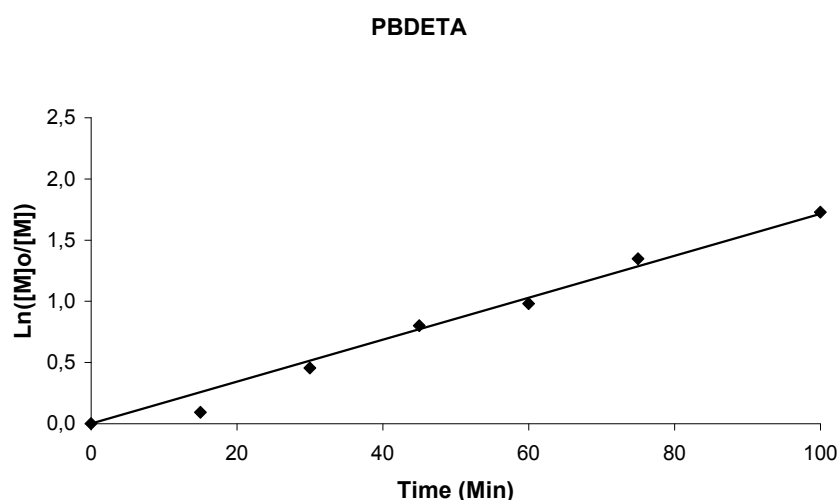


Figure 4.23 Semi-logarithmic kinetic plot for ATRP of MMA using PBDETA as a ligand. $[M]_0/[I]_0/[CuBr]_0/[PBDETA]_0=200/1/1/1$. $[MMA]=6,24 \text{ mol l}^{-1}$ in anisole (50 % V/V) at 80°C.

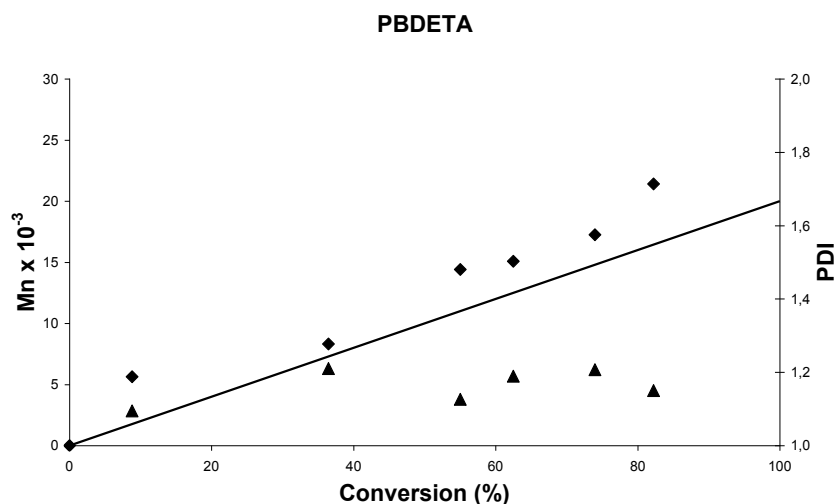


Figure 4.24 Molecular weight and molecular weight distribution versus conversion plot for ATRP of MMA using PBDETA (♦: Mn, ▲: PDI). [MMA]=6,24 mol l⁻¹ in anisole (50 % V/V) at 80°C. [M]₀/[I]₀/[CuBr]₀/[PBDETA]₀=200/1/1/1.

4.3.3. Using 1,1,4,7,7-pentahexyldiethylenetriamine (PHDETA)

The semi-logarithmic kinetic plot ($\ln([M]_0/[M])$ versus time) of ATRP reaction of MMA was shown in Figure 4.25 A straight line is observed indicating that the kinetics is first order with respect to the monomer concentration in the polymerization and demonstrates that active center concentration is constant during the polymerization. This result explains that termination is absent or negligible. Apparent rate constant of MMA polymerization using PHDETA at 80 °C was calculated from the figure as $k_{app}=2,75 \times 10^{-4} \text{ s}^{-1}$.

Molecular weight of the polymer versus conversion plot was shown in Figure 4.26 linear relationship indicates that transfer reactions are absent or insignificant. Measured molecular weights of the polymer are found close to theoretical ones.

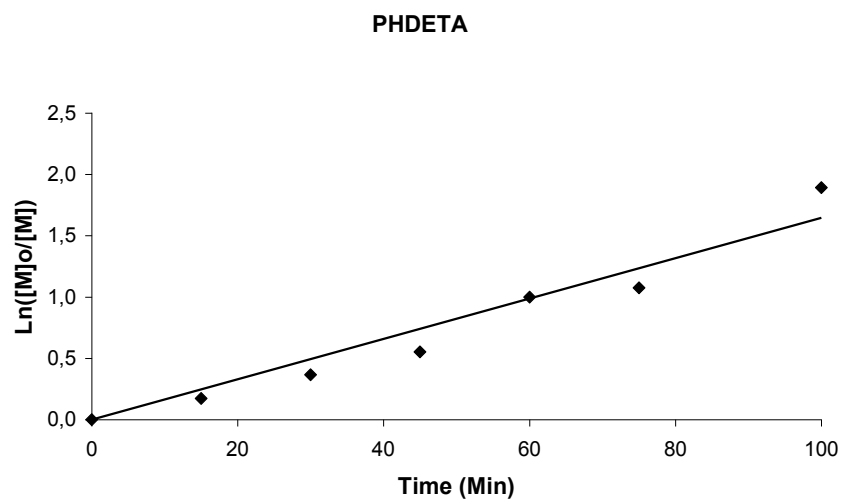


Figure 4.25 Semi-logarithmic kinetic plot for ATRP of MMA using PHDETA as a ligand. $[M]_0/[I]_0/[CuBr]_0/[PHDETA]_0=200/1/1/1$. $[MMA]=6,24 \text{ mol l}^{-1}$ in anisole (50 % V/V) at 80°C .

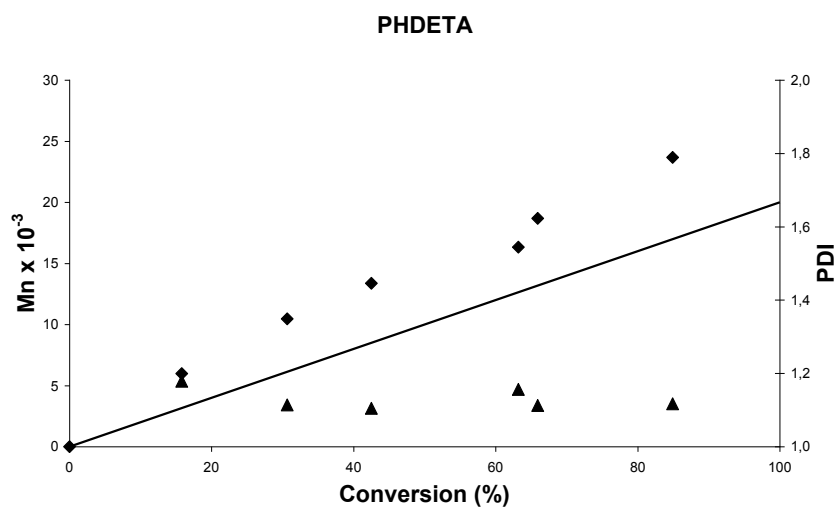


Figure 4.26 Molecular weight and molecular weight distribution versus conversion plot for ATRP of MMA using PHDETA (♦: Mn, ▲: PDI). $[MMA]=6,24 \text{ mol l}^{-1}$ in anisole (50 % V/V) at 80°C . $[M]_0/[I]_0/[CuBr]_0/[PHDETA]_0=200/1/1/1$.

4.3.4. Using 1,1,4,7,10,10-hexaethyltriethylenetetramine (HETETA)

The semi-logarithmic kinetic plot ($\ln([M]_0/[M])$ versus time) of ATRP reaction of MMA was shown in Figure 4.27. A straight line is observed indicating that the kinetics is first order with respect to the monomer concentration in the polymerization and demonstrates that active center concentration is constant during the polymerization. This result explains that termination is absent or negligible. Apparent rate constant of MMA polymerization using HETETA at 80 °C was calculated from the figure as $k_{app}=2,63 \times 10^{-4} \text{ s}^{-1}$.

Molecular weight of the polymer versus conversion plot was shown in Figure 4.28. A linear relationship indicates that transfer reactions are absent or insignificant. Measured molecular weights of the polymer are found close to theoretical ones.

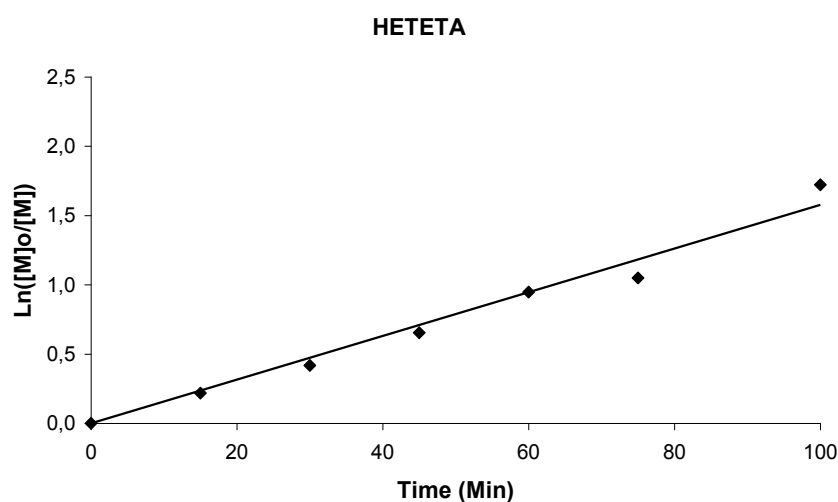


Figure 4.27 Semi-logarithmic kinetic plot for ATRP of MMA using HETETA as a ligand. $[M]_0/[I]_0/[CuBr]_0/[HETETA]_0=200/1/1/1$. $[MMA]=6,24 \text{ mol l}^{-1}$ in anisole (50 % V/V) at 80°C.

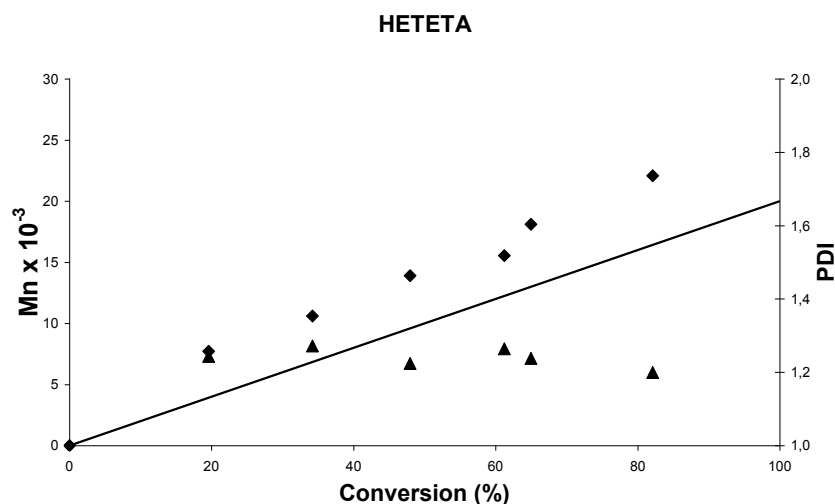


Figure 4.28 Molecular weight and molecular weight distribution versus conversion plot for ATRP of MMA using HETETA (◆: Mn, ▲: PDI). [MMA]=6,24 mol l⁻¹ in anisole (50 % V/V) at 80°C. [M]₀/[I]₀/[CuBr]₀/[HETETA]₀=200/1/1/1.

4.3.5. Using 1,1,4,7,10,10-hexabutyl triethylenetetramine (HBTETA)

The semi-logarithmic kinetic plot ($\ln([M]_0/[M])$ versus time) of ATRP reaction of MMA was shown in Figure 4.29 A straight line is observed indicating that the kinetics is first order with respect to the monomer concentration in the polymerization and demonstrates that active center concentration is constant during the polymerization. This result explains that termination is absent or negligible. Apparent rate constant of MMA polymerization using HBTETA at 80 °C was calculated from the figure as $k_{app}=2,42 \times 10^{-4} \text{ s}^{-1}$.

Molecular weight of the polymer versus conversion plot was shown in Figure 4.30 linear relationship indicates that transfer reactions are absent or insignificant. Measured molecular weights of the polymer are found close to theoretical ones.

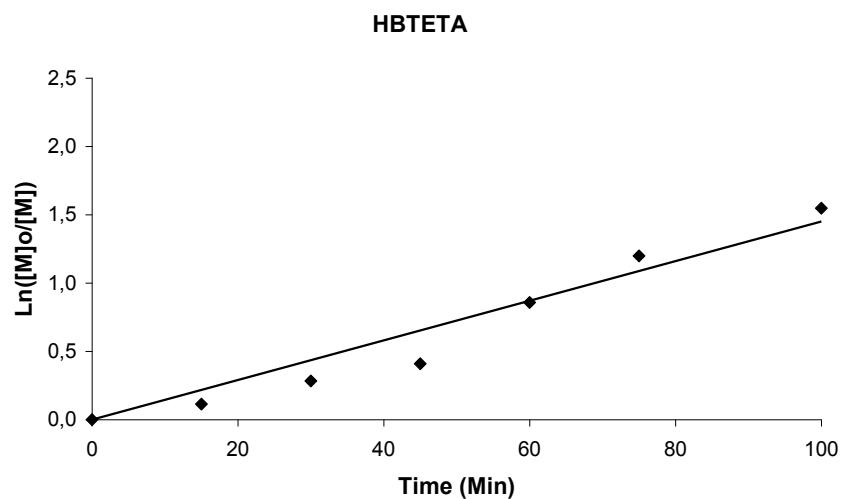


Figure 4.29 Semi-logarithmic kinetic plot for ATRP of MMA using HBTETA as a ligand. $[M]_0/[I]_0/[CuBr]_0/[HBTETA]_0=200/1/1/1$. $[MMA]=6,24 \text{ mol l}^{-1}$ in anisole (50 % V/V) at 80°C .

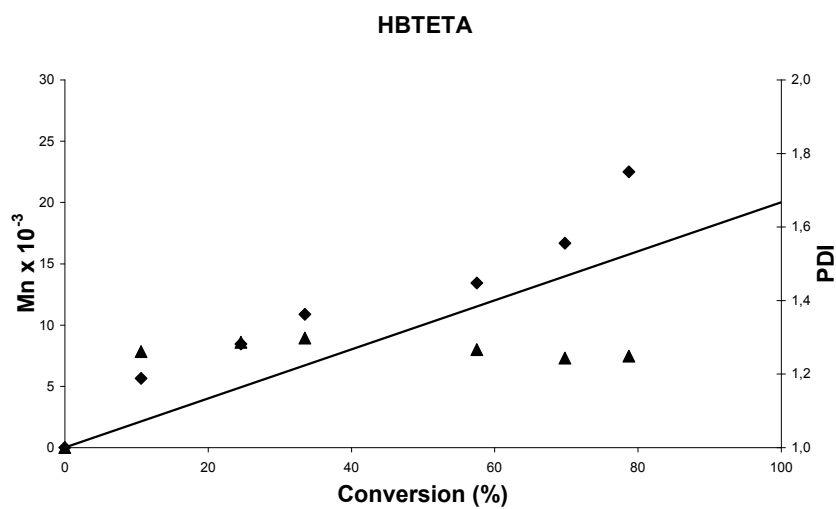


Figure 4.30 Molecular weight and molecular weight distribution versus conversion plot for ATRP of MMA using HBTETA (♦: Mn, ▲: PDI). $[MMA]=6,24 \text{ mol l}^{-1}$ in anisole (50 % V/V) at 80°C . $[M]_0/[I]_0/[CuBr]_0/[HBTETA]_0=200/1/1/1$.

4.3.6. Using 1,1,4,7,10,10-hexahexyltriethylenetetramine (HHTETA)

The semi-logarithmic kinetic plot ($\ln([M]_0/[M])$ versus time) of ATRP reaction of MMA was shown in Figure 4.31. A straight line is observed indicating that the kinetics is first order with respect to the monomer concentration in the polymerization and demonstrates that active center concentration is constant during the polymerization. This result explains that termination is absent or negligible. Apparent rate constant of MMA polymerization using HHTETA at 80 °C was calculated from the figure as $k_{app}=2,17 \times 10^{-4} \text{ s}^{-1}$.

Molecular weight of the polymer versus conversion plot was shown in Figure 4.32. A linear relationship indicates that transfer reactions are absent or insignificant. Measured molecular weights of the polymer are found close to theoretical ones.

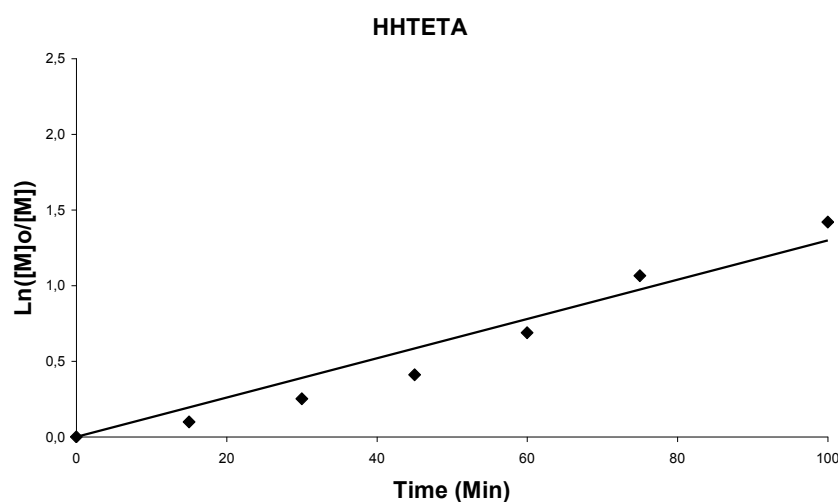


Figure 4.31 Semi-logarithmic kinetic plot for ATRP of MMA using HHTETA as a ligand. $[M]_0/[I]_0/[CuBr]_0/[HHTETA]_0=200/1/1/1$. $[MMA]=6,24 \text{ mol l}^{-1}$ in anisole (50 % V/V) at 80°C.

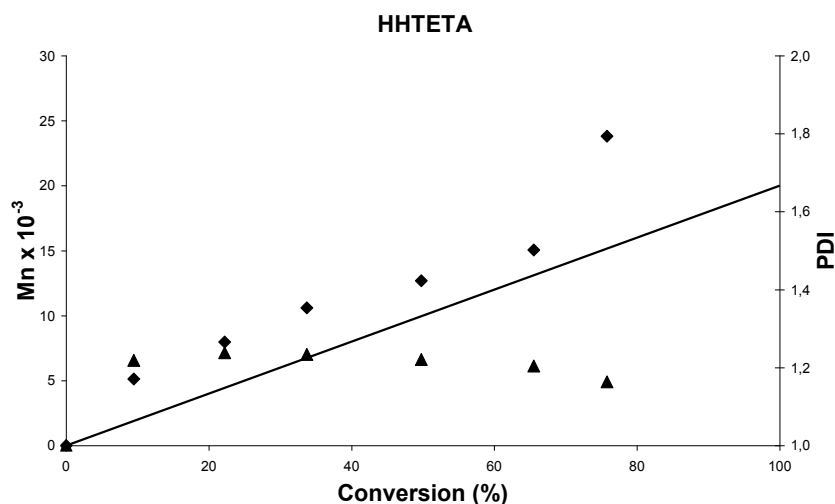


Figure 4.32 Molecular weight and molecular weight distribution versus conversion plot for ATRP of MMA using HHTETA (\blacklozenge : Mn, \blacktriangle : PDI). $[MMA]=6,24 \text{ mol l}^{-1}$ in anisole (50 % V/V) at 80°C . $[M]_0/[I]_0/[CuBr]_0/[HHTETA]_0=200/1/1/1$.

4.3.7. Using 1,1,4,7,7-pentamethyldiethylenetriamine (PMDETA)

The semi-logarithmic kinetic plot ($\ln([M]_0/[M])$ versus time) of ATRP reaction of MMA was shown in Figure 4.33 A straight line is observed indicating that the kinetics is first order with respect to the monomer concentration in the polymerization and demonstrates that active center concentration is constant during the polymerization. This result explains that termination is absent or negligible. Apparent rate constant of MMA polymerization using PMDETA at 80°C was calculated from the figure as $k_{app}=2,30 \times 10^{-4} \text{ s}^{-1}$.

Molecular weight of the polymer versus conversion plot was shown in Figure 4.34 linear relationship indicates that transfer reactions are absent or insignificant. Measured molecular weights of the polymer are found close to theoretical ones.

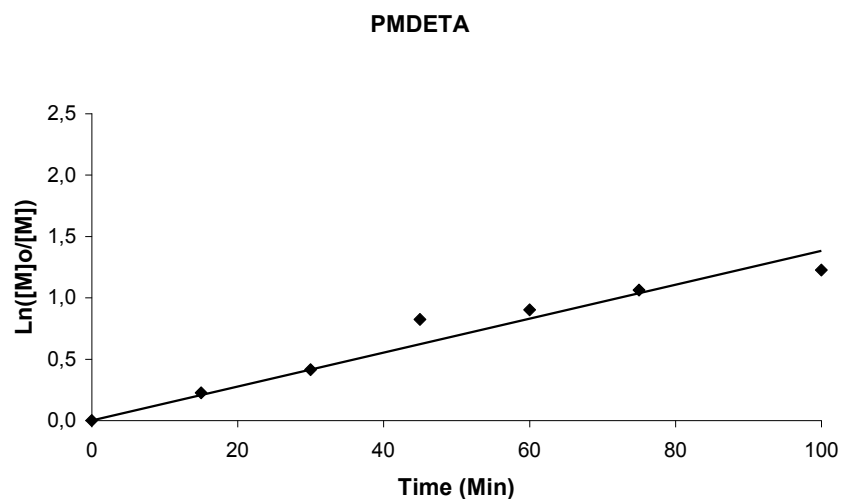


Figure 4.33 Semi-logarithmic kinetic plot for ATRP of MMA using PMDETA as a ligand. $[M]_0/[I]_0/[CuBr]_0/[PMDETA]_0=200/1/1/1$. $[MMA]=6,24 \text{ mol l}^{-1}$ in anisole (50 % V/V) at 80°C .

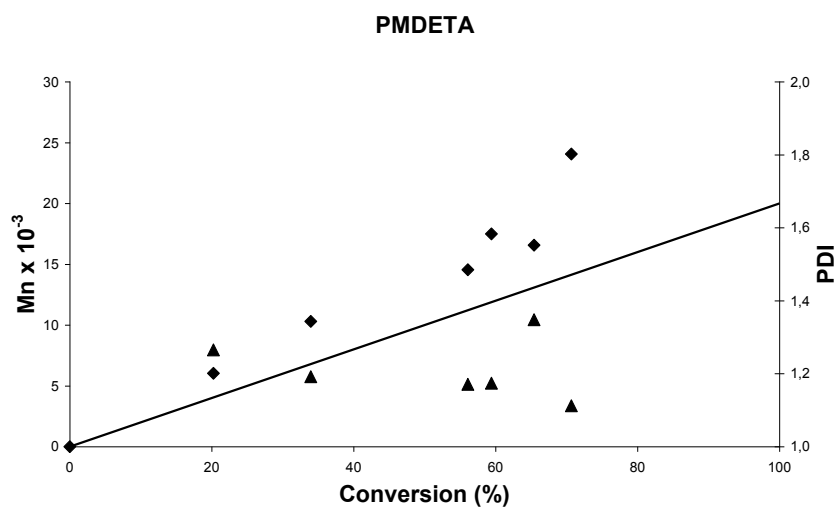


Figure 4.34 Molecular weight and molecular weight distribution versus conversion plot for ATRP of MMA using PMDETA (♦: M_n , ▲: PDI). $[MMA]=6,24 \text{ mol l}^{-1}$ in anisole (50 % V/V) at 80°C . $[M]_0/[I]_0/[CuBr]_0/[PMDETA]_0=200/1/1/1$.

4.3.8. Using bipyridine (bpy)

The semi-logarithmic kinetic plot ($\ln([M]_0/[M])$ versus time) of ATRP reaction of MMA was shown in Figure 4.35. A straight line is observed indicating that the kinetics is first order with respect to the monomer concentration in the polymerization and demonstrates that active center concentration is constant during the polymerization. This result explains that termination is absent or negligible. Apparent rate constant of MMA polymerization using bpy at 80 °C was calculated from the figure as $k_{app}=1,88 \times 10^{-4} \text{ s}^{-1}$.

Molecular weight of the polymer versus conversion plot was shown in Figure 4.36. A linear relationship indicates that transfer reactions are absent or insignificant. Measured molecular weights of the polymer are found close to theoretical ones.

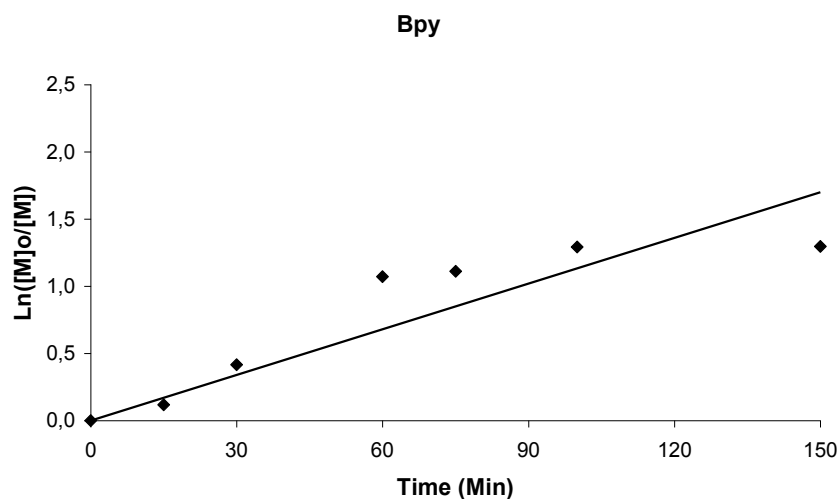


Figure 4.35 Semi-logarithmic kinetic plot for ATRP of MMA using bpy as a ligand. $[M]_0/[I]_0/[CuBr]_0/[bpy]_0=200/1/1/1$. $[MMA]=6,24 \text{ mol l}^{-1}$ in anisole (50 % V/V) at 80°C.

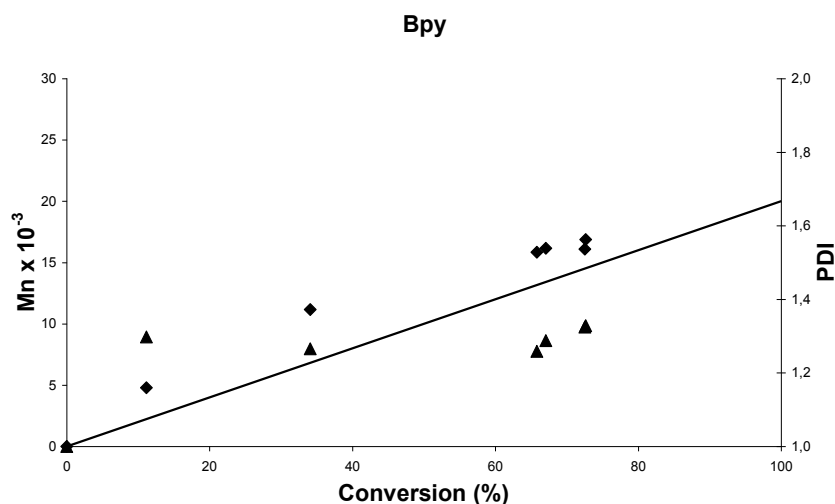


Figure 4.36 Molecular weight and molecular weight distribution versus conversion plot for ATRP of MMA using bpy (◆: Mn, ▲: PDI). [MMA]=6,24 mol l⁻¹ in anisole (50 % V/V) at 80°C. [M]₀/[I]₀/[CuBr]₀/[bpy]₀=200/1/1/1.

4.3.9. Using dinonylbipyridine (dNbpy)

The semi-logarithmic kinetic plot ($\ln([M]_0/[M])$ versus time) of ATRP reaction of MMA was shown in Figure 4.37 A straight line is observed indicating that the kinetics is first order with respect to the monomer concentration in the polymerization and demonstrates that active center concentration is constant during the polymerization. This result explains that termination is absent or negligible. Apparent rate constant of MMA polymerization using dNbpy at 80 °C was calculated from the figure as $k_{app}=0,42 \times 10^{-4} \text{ s}^{-1}$.

Molecular weight of the polymer versus conversion plot was shown in Figure 4.38 linear relationship indicates that transfer reactions are absent or insignificant. Measured molecular weights of the polymer are found close to theoretical ones.

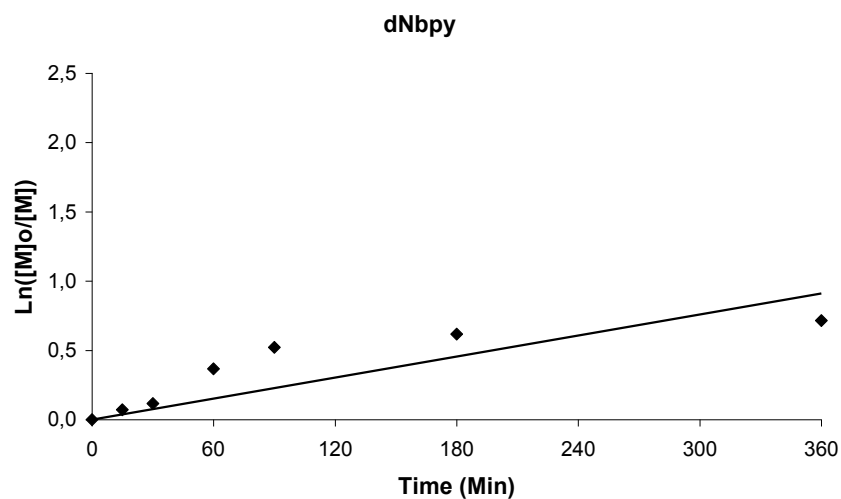


Figure 4.37 Semi-logarithmic kinetic plot for ATRP of MMA using dNbpy as a ligand. $[M]_0/[I]_0/[CuBr]_0/[dNbpy]_0=200/1/1/1$. $[MMA]=6,24 \text{ mol l}^{-1}$ in anisole (50 % V/V) at 80°C .

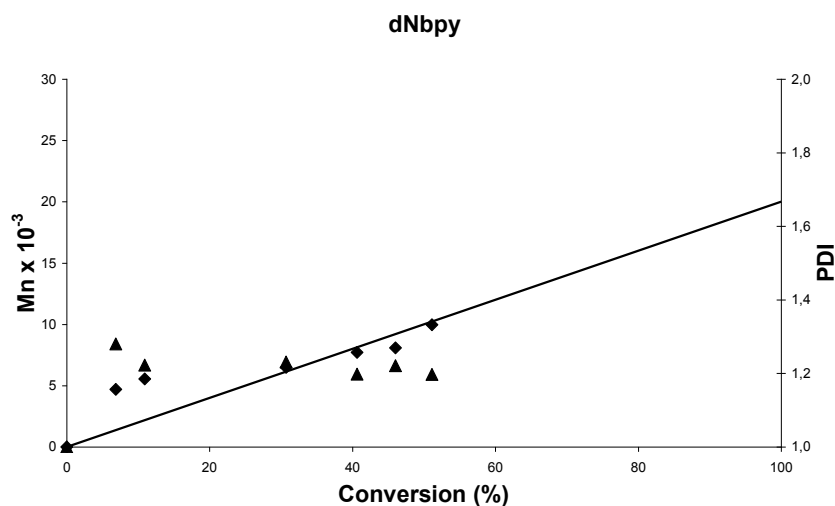


Figure 4.38 Molecular weight and molecular weight distribution versus conversion plot for ATRP of MMA using dNbpy (♦: M_n , ▲: PDI). $[MMA]=6,24 \text{ mol l}^{-1}$ in anisole (50 % V/V) at 80°C . $[M]_0/[I]_0/[CuBr]_0/[dNbpy]_0=200/1/1/1$.

4.3.10. Using (2-(dimethylamino)-ethyl)amine (Me₆-TREN)

The semi-logarithmic kinetic plot ($\ln([M]_0/[M])$ versus time) of ATRP reaction of MMA was shown in Figure 4.39 A straight line is observed indicating that the kinetics is first order with respect to the monomer concentration in the polymerization and demonstrates that active center concentration is constant during the polymerization. This result explains that termination is absent or negligible. Apparent rate constant of MMA polymerization using Me₆-TREN at 80 °C was calculated from the figure as $k_{app}=1,27 \times 10^{-4} \text{ s}^{-1}$.

Molecular weight of the polymer versus conversion plot was shown in Figure 4.40 linear relationship indicates that transfer reactions are absent or insignificant.

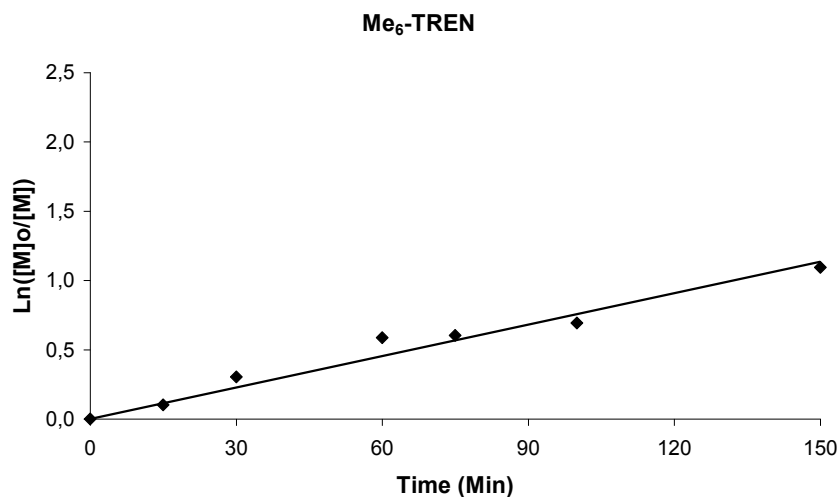


Figure 4.39 Semi-logarithmic kinetic plot for ATRP of MMA using Me₆-TREN as a ligand. $[M]_0/[I]_0/[CuBr]_0/[Me_6-TREN]_0=200/1/1/1$. $[MMA]=6,24 \text{ mol l}^{-1}$ in anisole (50 % V/V) at 80°C.

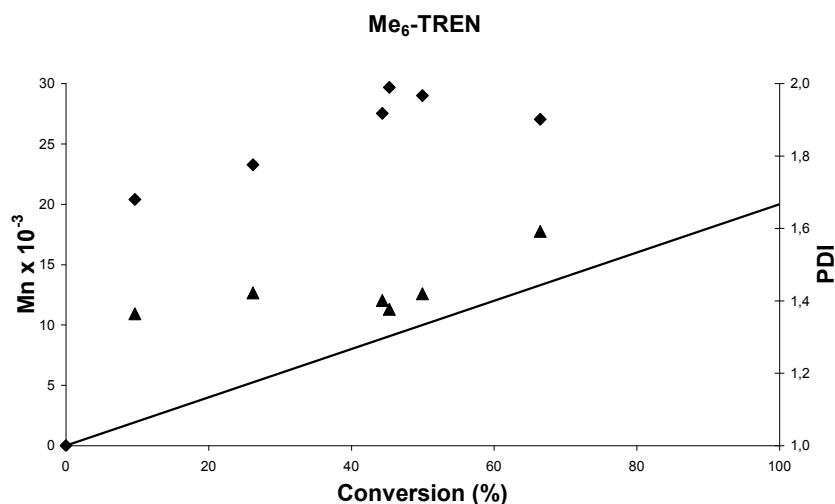


Figure 4.40 Molecular weight and molecular weight distribution versus conversion plot for ATRP of MMA using Me₆-TREN (◆: Mn, ▲: PDI). [MMA]=6,24 mol l⁻¹ in anisole (50 % V/V) at 80°C. [M]₀/[I]₀/[CuBr]₀/[Me₆-TREN]₀=200/1/1/1.

4.4. Results for ATRP of Methyl Methacrylate

Ten experiments performed for ATRP of MMA in conditions explained above. For each of the experiment;

- Rate of polymerization (R_p) calculated from semi-logarithmic kinetic plot,
- M_n and M_w of polymers measured by GPC method,
- Initiator efficiencies are calculated using theoretical M_n and measured M_n values,
- Polymers with low polydispersity index (PDI) are obtained.

Results collected from these ten experiments and results from a reference [2], are shown in Table 4.2.

Table 4.2. Results for ATRP of MMA in carried out experiments

Ligand	Time (min)	Conv * (%)	$M_{n,Cat}$	$M_{n,GPC}^*$	PDI*	R_p ($10^{-4} s^{-1}$)	Ini Eff. (f)
PEDETA^a	100	84	16800	23700	1,21	3,30	0,71
PBDETA^a	100	82	16400	21400	1,15	2,85	0,72
PHDETA^a	100	85	17000	23600	1,11	2,75	0,74
HETETA^a	100	82	16400	22100	1,19	2,63	0,74
HBTETA^a	100	79	16800	22500	1,24	2,42	0,75
HHTETA^a	100	76	16200	23800	1,16	2,17	0,68
PMDETA^a	100	71	14200	24000	1,11	2,30	0,60
bpy^a	150	73	14600	16800	1,33	1,88	0,87
dNbpy^a	360	51	10200	9900	1,20	0,42	1,00
Me₆TREN^a	150	67	13400	27000	1,59	1,27	0,49
HHTETA^{b,1}	120	65	19500	23000	1,18	1,1	0,85

^a [MMA]=6,24 mol l⁻¹ in anisole (50 % V/V) at 80 °C. [M]_o/[I]_o/[CuBr]_o/[ligand]_o=200/1/1/1

^b [MMA]=9,36 mol l⁻¹ (bulk) at 75 °C. [M]_o/[EBP]_o/[CuBr]_o/[HHTETA]_o=300/1/1/1

¹ Ref. [2]

* Last point of kinetic data

In these ATRP reactions homogeneity has been achieved by using PEDETA, PBDETA, PHDETA, HETETA, HBTETA, HHTETA and dNbpy ligands. PEDETA has the highest R_p for MMA in examined ligands. R_p has been decreased by increasing of the alkyl chain length for both linear tridentate and tetradentate linear amine ligands.

4.5. Comparison of Ligands

In this study three different ATRP conditions from literature [23,52] are repeated and also ATRP reactions using PEDETA and HETETA in these conditions are performed.

ATRP of MMA performed with PMDETA, PEDETA and HETETA in same conditions which were given in reference [23] for PMDETA. Conditions are as follows, $[MMA]=4,92 \text{ mol l}^{-1}$ in anisol (100 % V/V) at $90 \text{ }^\circ\text{C}$, $[MMA]_o/[EiBB]_o/[CuBr]_o/[ligand]_o = 200/1/1/1$.

The semi-logarithmic kinetic plots ($\ln([M]_o/[M])$ versus time) of ATRP reactions of MMA was shown in Figure 4.41 . k_{app} for PMDETA given in reference is $1,77 \times 10^{-4} \text{ s}^{-1}$, k_{app} values calculated from experiments are; for PMDETA $k_{app} = 2,3 \times 10^{-4} \text{ s}^{-1}$, for PEDETA $k_{app} = 2,52 \times 10^{-4} \text{ s}^{-1}$, for HETETA $k_{app} = 2,63 \times 10^{-4} \text{ s}^{-1}$.

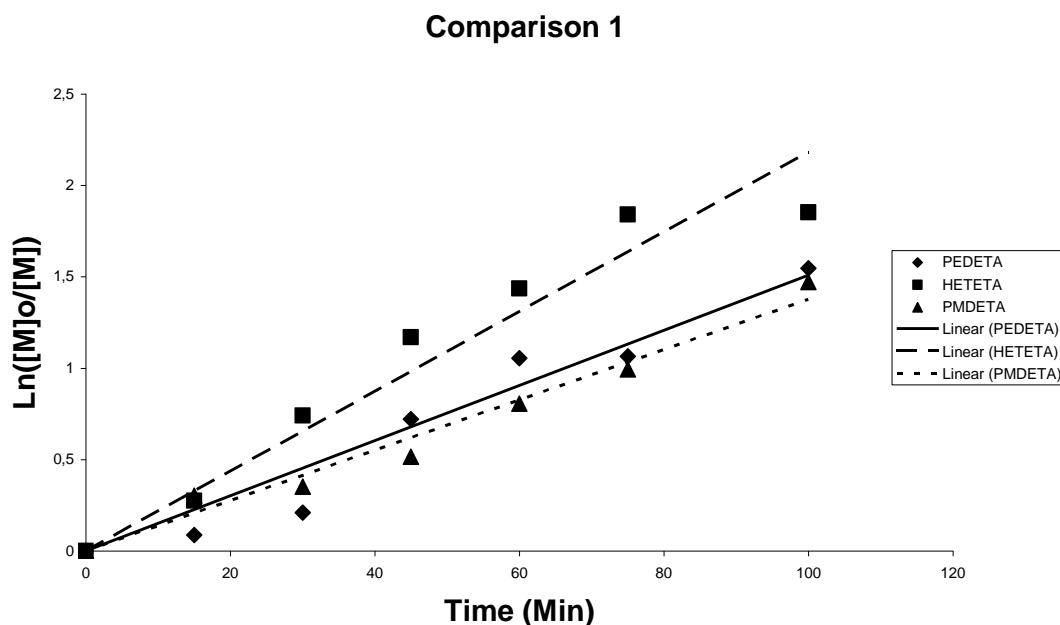


Figure 4.41 Semi-logarithmic kinetic plot for ATRP of MMA using PMDETA, PEDETA, HETETA as ligand. $[M]_o/[I]_o/[CuBr]_o/[ligand]_o = 200/1/1/1$. $[MMA]=4,92 \text{ mol l}^{-1}$ in anisole (100 % V/V) at 90°C .

ATRP of St performed with PMDETA, PEDETA and HETETA in same conditions which were given in reference [23] for PMDETA. Conditions are as follows, $[St]=8,7 \text{ mol l}^{-1}$ (bulk) at $110 \text{ }^\circ\text{C}$, $[St]_0/[1\text{-PEBr}]_0/[CuBr]_0/[ligand]_0 = 96/1/1/1$.

The semi-logarithmic kinetic plots ($\ln([M]_0/[M])$ versus time) of ATRP reactions of St was shown in Figure 4.42 . k_{app} for PMDETA given in reference is $3,58 \times 10^{-4} \text{ s}^{-1}$, k_{app} values for experiments done are; for PMDETA $k_{app} = 1,88 \times 10^{-4} \text{ s}^{-1}$, for PEDETA $k_{app} = 3,22 \times 10^{-4} \text{ s}^{-1}$, for HETETA $k_{app} = 3,13 \times 10^{-4} \text{ s}^{-1}$.

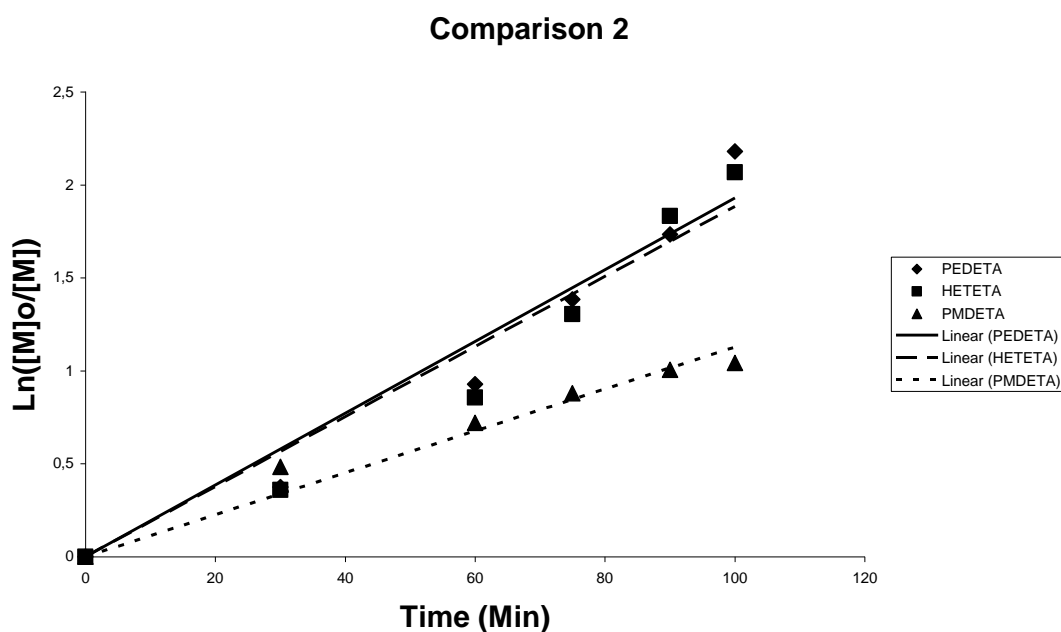


Figure 4.42 Semi-logarithmic kinetic plot for ATRP of St using PMDETA, PEDETA, HETETA as ligand. $[M]_0/[I]_0/[CuBr]_0/[ligand]_0 = 96/1/1/1$. $[St]=8,7 \text{ mol l}^{-1}$ (bulk) at 110°C .

ATRP of St performed with Me₆-TREN, PEDETA and HETETA in same conditions which were given in reference [52] for Me₆-TREN. Conditions are as follows, [St]₀=8,73 mol l⁻¹ (bulk) at 110 °C, [St]₀/[MBP]₀/[CuBr]₀/[ligand]₀ = 200/1/0,5/0,5

The semi-logarithmic kinetic plots (ln([M]₀/[M]) versus time) of ATRP reactions of St was shown in Figure 4.43 . k_{app} for Me₆-TREN given in reference is $0,62 \times 10^{-4} \text{ s}^{-1}$, k_{app} values for experiments done are; for Me₆-TREN $k_{app} = 0,56 \times 10^{-4} \text{ s}^{-1}$, for PEDETA $k_{app} = 0,88 \times 10^{-4} \text{ s}^{-1}$, for HETETA $k_{app} = 0,93 \times 10^{-4} \text{ s}^{-1}$.

Comparison 3

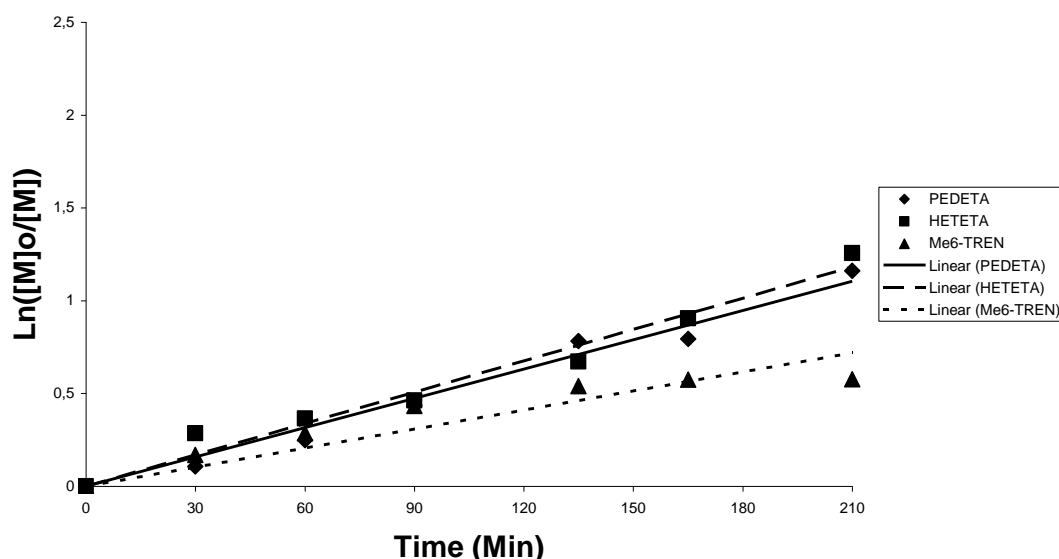


Figure 4.43 Semi-logarithmic kinetic plot for ATRP of St using Me₆-TREN, PEDETA, HETETA as ligand. [M]₀/[I]₀/[CuBr]₀/[ligand]₀ = 200/1/0,5/0,5. [St]=8,73 mol l⁻¹ (bulk) at 110°C.

Ethylated tridentate and tetradentate linear amine ligands provides faster polymerization rates compared to widely used ligands in conditions taken from literature.

5. CONCLUSION AND RECOMENDATIONS

Homogeneous ATRP reaction conditions are obtained by using 1,1,4,7,7-pentaethyldiethylenetriamine (PEDETA), 1,1,4,7,7-pentabutyl-diethylenetriamine (PBDETA), 1,1,4,7,7-pentahexyldiethylenetriamine (PHDETA), 1,1,4,7,10,10-hexaethyltriethylenetetramine (HETETA), 1,1,4,7,10,10-hexabutyltriethylene tetramine (HBTETA), 1,1,4,7,10,10-hexahexyltriethylenetetramine (HHTETA) for ATRP of St and MMA.

It was previously claimed that the activity of N-based ligands in ATRP decreases with the number of coordinating sites: $N_4 > N_3 > N_2 > N_1$ in the heterogeneous system [20]. In our study we have also observed the same trend for homogeneous St polymerization ($N_4 > N_3$). However, for the homogeneous MMA polymerization the order of activity was reverse ($N_4 < N_3$). The activity of DETA and TETA derivatives decreases with the increasing length of the alkyl chain ($C_2 > C_3 > C_4 > C_5 > C_6$), which may be due to the steric hindrance.

The ATRP by using alkylated linear amine ligands can be performed under homogeneous conditions and relatively fast polymerization rates were attained. Systematic investigation showed that by changing methyl group of PMDETA to ethyl introduces homogeneity to the polymerization system.

REFERENCES

- [1] **Matyjaszewski, K., Xia, J.**, 2001. *J. Chem Rev*, **101**, 2921–2990.
- [2] **Acar, M. H., Bicak, N.**, 2003. *Journal Of Polymer Science Part A-Polymer Chemistry*, **41**, 1677-1680.
- [3] **Xia, J., Zhang, X., Matyjaszewski, K.**, 2000. In *Transition Metal Macromolecular Design*, Boffa, L. S., Novak, B. M., Eds., ACS Symposium Series 760, American Chemical Society: Washington, DC, pp 207–223.
- [4] **Allcock, H. R., Lampe, F. W.**, 1990. *Contemporary Polymer Chemistry*. Prentice Hall: New Jersey, 2nd Ed., chapter 3.
- [5] **Matyjaszewski, K.**, 1994. *J. Macromol. Sci., Pure Appl. Chem.* **A31**, 989.
- [6] **Matyjaszewski, K., Sigwalt, P.**, 1994. *Polym. Int.* **35**, 1.
- [7] **Solomon, D. H., Rizzardo, E. and Cacioli, P.**, 1986. U.S. Patent 4,581,429.
- [8] **Kato, M., Kamigaito, M., Sawamoto, M. and Higashimura, T.**, 1995. *Macromolecules*, **28**, 1721.
- [9] **Wang, J. S., Matyjaszewski, K.**, 1995. *Macromolecules*, **28**, 7901–7910.
- [10] **Wang, J. S., Matyjaszewski, K.**, 1995. *J. Am. Chem. Soc.*, **117**, 5614–5615.
- [11] **Percec, V., Barboiu, B.**, 1995. *Macromolecules*, **28**, 7970–7972.
- [12] **Matyjaszewski, K.**, 1998. Ed. *Controlled Radical Polymerization*, ACS Symposium Series No. 685, American Chemical Society: Washington, DC.
- [15] **Matyjaszewski, K.**, 2000. Ed. *Controlled/Living Radical Polymerization. Progress in ATRP, NMP, and RAFT*, ACS Symposium Series No. 768, American Chemical Society: Washington, DC.
- [16] **Patten, T. E., Matyjaszewski, K.**, 1998. *Adv. Mater.*, **10**, 901.
- [17] **Matyjaszewski, K.**, 1999. *Chem. Eur. J.*, **5**, 3095.

- [18] **Patten, T. E., Matyjaszewski, K.**, 1999. *Acc. Chem. Res.*, **32**, 895–903.
- [19] **Kamigaito, M., Ando, T., Sawamoto, M.**, 2001. *Chem. Rev.*, **101**, 3689–3746.
- [20] **Matyjaszewski, K., Xia, J.**, 2002. In *Handbook of Radical Polymerization*, Matyjaszewski, K., Davis, T. P., Eds., Wiley: New York, p 602.
- [21] **Davis, K.A., Matyjaszewski, K.**, 2000. *Macromolecules*, **33**, 4039.
- [22] **Matyjaszewski, K.**, 2003. *Macromol.Symp.***195**,25-31.
- [23] **Xia, J., Matyjaszewski, K.**, 1997. *Macromolecules*, **30**, 7697–7700.
- [24] **Xia, J. H., Matyjaszewski, K.**, 1997. *Macromolecules*, **30**, 7692–7696.
- [25] **Wang, J. L., Grimaud, T., Matyjaszewski, K.**, 1997. *Macromolecules*, **30**, 6507–6512.
- [26] **Kickelbick, G., Matyjaszewski, K.**, 1999. *Macromol Rapid Commun*, **20**, 341–346.
- [27] **Matyjaszewski, K., Goebelt, B., Paik, H.-J., Horwitz, C. P.**, 2001. *Macromolecules*, **34**, 430–440.
- [28] **Destarac, M., Bessiere, J.-M., Boutevin, B.**, 1997. *Macromol Rapid Commun*, **18**, 967–974.
- [29] **Xia, J., Matyjaszewski, K.**, 1999. *Macromolecules*, **32**, 2434–2437.
- [30] **Haddleton, D. M., Jasiieczek, C. B., Hannon, M. J., Shooter, A. J.**, 1997. *Macromolecules*, **30**, 2190–2193.
- [31] **Amass, A. J., Wyres, C. A., Colclough, E., Hohn, I. M.**, 2000. *Polymer*, **41**, 1697–1702.
- [32] **Haddleton, D. M., Crossman, M. C., Dana, B. H., Duncalf, D. J., Heming, A. M., Kukulj, D., Shooter, A. J.**, 1999. *Macromolecules*, **32**, 2110–2119.

- [33] **Clark, A. J., Battle, G. M., Heming, A. M., Haddleton, D. M., Bridge, A.,** 2001. *Tetrahedron Lett*, **42**, 2003–2005.
- [34] **Wang, X. S., Malet, F. L. G., Armes, S. P., Haddleton, D. M., Perrier, S.,** 2001. *Macromolecules*, **34**, 162–164.
- [35] **Shen, Y., Zhu, S., Zeng, F., Pelton, R. H.,** 2000. *Macromol. Chem. Phys.*, **201**, 1169–1175.
- [36] **Shen, Y., Zhu, S., Pelton, R. H.,** 2001. *Macromolecules*, **34**, 3182–3185.
- [37] **Shen, Y., Zhu, S.,** 2001. *Macromolecules*, **34**, 8603–8609.
- [38] **Xia, J., Gaynor, S. G., Matyjaszewski, K.,** 1998. *Macromolecules*, **31**, 5958–5959.
- [39] **Gromada, J., Matyjaszewski, K.,** 2002. *Polym. Prepr. (Am. Chem. Soc. Div. Polym. Chem.)*, **43(2)**, 195–196.
- [40] **Shen, Y., Zhu, S.,** 2002. *AIChE J*, **48**, 2609–2619.
- [41] **Zeng, F., Shen, Y., Zhu, S., Pelton, R.,** 2000. *Macromolecules*, **33**, 1628–1635.
- [42] **Fischer, H.** 1999. *J. Polym. Sci., Part A: Polym. Chem.*, **37**, 1885.
- [43] **Fischer, H.,** 1997. *Macromolecules*, **30**, 5666.
- [44] **Shipp, D. A., Matyjaszewski, K.,** 2000. *Macromolecules*, **33**, 1553.
- [45] **Matyjaszewski, K., Patten, T. E., Xia, J.,** 1997. *J. Am. Chem. Soc.*, **119**, 674.
- [46] **Davis, K., Paik, H.-j., Matyjaszewski, K.,** 1999. *Macromolecules*, **32**, 1767.
- [47] **Percec, V., Barboiu, B., Kim, H.-J.,** 1998. *J. Am. Chem. Soc.*, **120**, 305.
- [48] **Percec, V., Barboiu, B., Neumann, A., Ronda,** 1996. *Macromolecules*, **29**, 3665.
- [49] **Levy, A. T., Olmstead, M. M., Patten, T. E.,** 2000. *Inorg. Chem.*, **39**, 1628.

[50] **Inceoglu, S., Olugebefola, S. C., Acar, M. H., Mayes, A. M.**, 2004. Des. Monomers Polym., **7**, 181-189.

[51] **Becer, C.R.**, 2005. Synthesis of Alkylated Linear Amine Ligands for homogeneous Atom Transfer Radical Polymerization, *M.Sc. Thesis*, I.T.U. Institute of Science and Technology.

[52] **Queffelec, J., Gaynor, S. G., Matyjaszewski, K.**, 2000. Macromolecules, **33**, 8629-8639.

AUTOBIOGRAPHY

He was born in 1979 in Istanbul. In 1997, he was graduated from Beşiktaş Atatürk Anadolu Highschool and registered to the Chemistry Department of Istanbul Technical University in same year.

After graduating from Istanbul Technical University in 2003, he was registered as a M.Sc. student to Istanbul Technical University, Polymer Science and Technology Department of the Institute of Science and Technology in 2003.